A framework for evaluation and characterization of drift prediction in the marine environment

Nancy Soontiens and Jennifer Holden

Fisheries and Oceans Canada
Science Branch, Newfoundland and Labrador Region
Environmental Sciences Division
Northwest Atlantic Fisheries Centre
80 East White Hills Road
St. John's, NL
A1C 5X1

2024

Canadian Technical Report of
Hydrography and Ocean Sciences 383

Fisheries and Oceans Canada | Pêches et Océans Canada

Canada

Canadian Technical Report of Hydrography and Ocean Sciences

Technical reports contain scientific and technical information of a type that represents a contribution to existing knowledge but which is not normally found in the primary literature. The subject matter is generally related to programs and interests of the Oceans and Science sectors of Fisheries and Oceans Canada.

Technical reports may be cited as full publications. The correct citation appears above the abstract of each report. Each report is abstracted in the data base *Aquatic Sciences and Fisheries Abstracts.*

Technical reports are produced regionally but are numbered nationally. Requests for individual reports will be filled by the issuing establishment listed on the front cover and title page.

Regional and headquarters establishments of Ocean Science and Surveys ceased publication of their various report series as of December 1981. A complete listing of these publications and the last number issued under each title are published in the *Canadian Journal of Fisheries and Aquatic Sciences*, Volume 38: Index to Publications 1981. The current series began with Report Number 1 in January 1982.

Rapport technique canadien sur l'hydrographie et les sciences océaniques

Les rapports techniques contiennent des renseignements scientifiques et techniques qui constituent une contribution aux connaissances actuelles mais que l'on ne trouve pas normalement dans les revues scientifiques. Le sujet est généralement rattaché aux programmes et intérêts des secteurs des Océans et des Sciences de Pêches et Océans Canada.

Les rapports techniques peuvent être cités comme des publications à part entière. Le titre exact figure au-dessus du résumé de chaque rapport. Les rapports techniques sont résumés dans la base de données *Résumés des sciences aquatiques et halieutiques*.

Les rapports techniques sont produits à l'échelon régional, mais numérotés à l'échelon national. Les demandes de rapports seront satisfaites par l'établissement auteur dont le nom figure sur la couverture et la page de titre.

Les établissements de l’ancien secteur des Sciences et Levés océaniques dans les régions et à l'administration centrale ont cessé de publier leurs diverses séries de rapports en décembre 1981. Vous trouverez dans l'index des publications du volume 38 du *Journal canadien des sciences halieutiques et aquatiques*, la liste de ces publications ainsi que le dernier numéro paru dans chaque catégorie. La nouvelle série a commencé avec la publication du rapport numéro 1 en janvier 1982.

Canadian Technical Report of Hydrography and Ocean Sciences 383

2024

A framework for evaluation and characterization of drift prediction in the marine environment

by

Nancy Soontiens, Jennifer Holden

Fisheries and Oceans Canada
Science Branch, Newfoundland and Labrador Region
Environmental Sciences Division
Northwest Atlantic Fisheries Centre
80 East White Hills Road
St. John's, NL
A1C 5X1

© His Majesty the King in Right of Canada, as represented by the Minister of the Department of Fisheries and Oceans, 2024.
Cat. Fs 97-18/383E-PDF ISBN 978-0-660-72811-7 ISSN 1488-5417

Correct citation for this publication:

Soontiens, N., and Holden, J. 2024. A framework for evaluation and characterization of drift prediction in the marine environment. Can. Tech. Rep. Hydrogr. Ocean Sci. 383: ix + 45 p.

Contents

List of Tables

List of Figures

ABSTRACT

Soontiens, N., and Holden, J. 2024. A framework for evaluation and characterization of drift prediction in the marine environment. Can. Tech. Rep. Hydrogr. Ocean Sci. 383: ix + 45 p.

As part of the Oceans Protection Plan (OPP), the Government of Canada initiated several programs to support marine environmental emergency response. This report describes a project under OPP to develop drift prediction and verification tools for surface and subsurface drifting objects. The goal of this project is to establish a framework that enables comparison of drift predictions with observed drift trajectories using a standard set of evaluation metrics and outputs. This framework provides a consistent and streamlined environment for generating predicted drift trajectories forced with a variety of model inputs and solved with a number of numerical integration techniques. In addition to direct comparisons with observed drift trajectories, this framework can produce drift predictions to visualize and describe ocean circulation patterns. Moreover, methods for direct comparison between ocean model currents and currents derived from observed drifters are provided in the package. The framework itself is a modular, open source Python package. This report describes the framework, the methods applied when generating drift predictions, and several examples of how the framework can be used.

RÉSUMÉ

Soontiens, N., and Holden, J. 2024. A framework for evaluation and characterization of drift prediction in the marine environment. Can. Tech. Rep. Hydrogr. Ocean Sci. 383: ix + 45 p.

Dans le cadre du Plan de protection des océans (PPO), le gouvernement du Canada a lancé plusieurs programmes visant à soutenir les interventions d'urgence dans le domaine de l'environnement marin. Ce rapport décrit un projet du PPO visant à développer des outils de prédiction et de vérification de la dérive pour les objets dérivants de surface et de subsurface. L'objectif de ce projet est d'établir un cadre qui permet de comparer les prévisions de dérive avec les trajectoires de dérive observées en utilisant un ensemble standard de mesures d'évaluation et de résultats. Ce cadre fournit un environnement cohérent et rationalisé pour générer des trajectoires de dérive prédites forcées avec une variété d'entrées de modèle et résolues avec un certain nombre de techniques d'intégration numérique. Outre les comparaisons directes avec les trajectoires de dérive observées, ce cadre peut produire des prévisions de dérive pour visualiser et décrire les schémas de circulation océanique. En outre, des méthodes de comparaison directe entre les courants des modèles océaniques et les courants dérivés des dériveurs observés sont disponibles. Le cadre lui-même est un paquet de programmes modulaires écrits en Python et open source. Ce rapport décrit la structure, les méthodes appliquées lors de la génération des prévisions de dérive, et plusieurs exemples d'utilisation du cadre.

Acronyms

CIOPS-E Coastal Ice Ocean Prediction System for the East Coast of Canada

CIOPS-W Coastal Ice Ocean Prediction System for the West Coast of Canada

ECCC Environment and Climate Change Canada

GIOPS Global Ice Ocean Prediction System

HRDPS High Resolution Deterministic Prediction System

IOS Institute of Ocean Sciences

MLDPn Modèle Lagrangien de Dispersion des Particules d'ordre n

NEMO Nucleus for European Modelling of the Ocean

OPP Oceans Protection Plan

SCT Surface Circulation Tracker

SVP Surface Velocity Program

TReX Tracer Release Experiment

1 Introduction

Many applications benefit from the ability to predict drift and dispersion in the marine environment, such as search and rescue, oil spill response, plastics and debris tracking, vessels adrift, etc. Advances in operational ocean forecasting have enabled real-time availability of the ocean, atmosphere, and wave data needed to support these drift predictions. Although these forecasts are available and extremely useful, they are also subject to a variety of errors, such as unresolved physics due to inadequate resolution, uncertainty in initial conditions and forcing conditions, and approximations and parametrizations of physical processes. For this reason, there is a need to understand the accuracy of drift predictions generated from these forecasts so that end users and response personnel can make informed decisions about their reliability and accuracy.

As part of the Oceans Protection Plan (OPP), the Government of Canada initiated several programs to support marine environmental emergency response. This report describes a project under OPP to develop drift prediction and verification tools for surface and subsurface drifting objects. The goal of this project is to establish a framework that enables comparison of drift predictions with observed drift trajectories using a standard set of evaluation metrics and outputs. This framework provides a consistent and streamlined environment for generating predicted drift trajectories forced with a variety of model inputs and solved with a number of numerical integration techniques. Additional analysis can then be performed to provide comparisons between prediction systems, drift methodologies, drifter types, regions, etc. The analysis can be further customized to better represent drifting object type by using tailored drift parameters and post-processing.

In addition to direct comparisons with observed drift tracks, predictions can be used to visualize and describe ocean circulation patterns using the drift characterization features of this framework. Moreover, methods for direct comparison between ocean model currents and currents derived from observed drift tracks can be applied, which can be used to study the variability of forcing conditions and parameter choices (Sutherland et al. 2020). The framework itself is a modular, open source Python package available at `https://gitlab.com/dfo-drift-projection/drift-workflow-tool/`. This work is part of a larger sub-initiative to improve drift prediction and near-shore modelling in support of oil spill response and electronic navigation (e.g. Paquin et al. 2020; Nudds et al. 2020; Hourston et al. 2021; Lin et al. 2022).

This report is not a manual for how to use this framework. Rather, it is a description of the methods used, the types of results that can be produced using this tool, and some discussion on how the results can be interpreted. The report is organized as follows. First, an overview of the methods and framework for drift verification and characterization are provided in section 2. Second, a set of examples is provided in section 3 and finally, a description of future work is provided in section 4. Additional details regarding the specific implementation of the framework can be found on the project's associated GitLab wiki page: `https://gitlab.com/dfo-drift-projection/drift-workflow-tool/-/wikis/home`.

2 Methods

When establishing a drift prediction, there are many choices that impact the results. For instance, the selection of forcing data, the choice of drift methodology, and the representation of physical processes such as wind and wave influence on the drifter are some examples. The goal of this framework is to enable the determination of the settings which lead to an accurate drift prediction. The framework has been built to allow the outcome of these different initial settings to be easily compared. This is accomplished by using a streamlined set of namelists or configuration files for initializing the drift simulations and then comparing the results using a standard set of evaluation metrics.

In this section, we describe the forces and equations that are applied when producing a drift prediction (section 2.1). In addition, we describe the three drift methodologies that are currently

implemented (section 2.2). Finally, we describe three of the functionalities or modules available within this framework (section 2.3).

2.1 Forces and Equations

The framework provides several options for the representation of the forces acting on a virtual drifter. Each of these options is described in the series of equations below. The framework primarily adopts a deterministic perspective on drift prediction, that is, drift positions can be determined without applying any randomness to the equations governing their movement. It should be noted, however, that there is a wealth of literature and research associated with probabilistic frameworks for estimating drift pathways (see van Sebille et al. 2018; Ullman et al. 2006) and these methodologies are not thoroughly accounted for in this framework.

First, the simplest equation is one in which the drifter velocity is equal to the ocean current velocity:

$$\frac{d\boldsymbol{x}}{dt} = \boldsymbol{u_o},\ \boldsymbol{x}(t_0) = \boldsymbol{x_0} \tag{1}$$

where $\boldsymbol{x}(t)$ is the drifter position as a function of time, $\boldsymbol{u_o}$ is the ocean current acting on the drifter, t_0 is the initial time and $\boldsymbol{x_0}$ is the drifter position at time t_0. Variables in bold represent vector quantities.

Many drifting objects, such as oil, ships, and some ocean drifters are influenced by both the ocean current and the winds. In these situations, the drifter position can be modelled as

$$\frac{d\boldsymbol{x}}{dt} = \boldsymbol{u_o} + \alpha\boldsymbol{u_{10}},\ \boldsymbol{x}(t_0) = \boldsymbol{x_0} \tag{2}$$

where $\boldsymbol{u_{10}}$ is the 10-metre atmospheric velocity and α is the wind drift factor, or the fraction of the 10-metre wind speed acting on the drifter in the direction of the wind. In general, there is some uncertainty around the parameter α for most drift predictions (Sutherland et al. 2020; Abascal et al. 2009) but a canonical value for oil spill simulations is typically around 0.03. Some ocean drifter configurations such as the Surface Velocity Program (SVP) and CODE/Davis are designed to limit the influence of the winds on the drifter motion. These designs tend to have a much smaller theoretical value of α (i.e., < 0.01) because they maximize the drag area ratio (i.e., the cross-sectional area of the drifter below the waterline to the area above the waterline multiplied by the drag coefficient of each section). Empirical methods for selecting α also exist by carefully analyzing simultaneous measurements of the drifting object positions, ocean currents, and wind speed and directions.

Yet, even an accurate representation of the wind influence on the drifter by carefully selecting α does not mean that all forces acting on the drifter are accounted for. An additional force due to the periodic motion of a wave field can be modelled as

$$\frac{d\boldsymbol{x}}{dt} = \boldsymbol{u_o} + \alpha'\boldsymbol{u_{10}} + \boldsymbol{u_s},\ \boldsymbol{x}(t_0) = \boldsymbol{x_0} \tag{3}$$

where $\boldsymbol{u_s}$ is the stokes drift velocity derived from the wave field. The stokes drift velocity is the net drift velocity in the direction of wave propagation experienced by a particle in a wave field (van den Bremer et al. 2018). Note the change in notation for the the wind drift factor from α to α'. This distinction is made because the value of the wind fraction should not be the same when stokes drift is included (equation 3) and when it is not (equation 2). Because the wave field and associated stokes drift velocities are often related to the atmospheric conditions, wave influences can be approximated by equation 2 using an empirical (as opposed to theoretical) determination of α. However, there is no general rule of thumb for translating α to α' because the wave conditions are highly dependent on the regional geography in addition to the atmospheric conditions.

There are several other conventions for representing the forces acting on a drifting object that aren't presented in this report or available in this framework (e.g. forces due to the drifter's inertia). There are

also other conventions for describing the wind influence on the drifting object. Notably, search and rescue applications typically utilize a Leeway approach where wind effects are represented by nine Leeway parameters and are empirically determined based on an object's drifting characteristics and shape (Breivik et al. 2012). In this strategy, wave effects are implicitly represented in the empirically determined Leeway parameters.

Lastly, sub-grid scale motions can be optionally included in each of equations 1 - 3 as follows

$$\frac{d\boldsymbol{x}}{dt} = \boldsymbol{f}(t) + \boldsymbol{u'}(t),\ \boldsymbol{x}(t_0) = \boldsymbol{x_0} \tag{4}$$

where $\boldsymbol{f}(t)$ represents the terms on the right hand side of equations 1 - 3 respectively and $\boldsymbol{u'}(t)$ represents a random number vector with each component selected from a normal distribution with standard deviation u_{rms} where rms means 'root mean square' and represents the strength of velocity fluctuations.

Finally, these equations are solved numerically using standard time stepping techniques for ordinary differential equations such as the forward Euler method or the 4th order Runge-Kutta method (see van Sebille et al. 2018, for example). The ocean velocity ($\boldsymbol{u_o}$), 10-metre atmospheric winds ($\boldsymbol{u_{10}}$), and stokes velocities ($\boldsymbol{u_s}$) must be sourced from gridded model data as inputs. The data from each model type does not have to be on the same grid because the drift methodology typically handles regridding and interpolation of velocity fields where needed. More information about how each drift methodology handles interpolation and rotation is provided in section 2.2.

2.2 Drift Methodologies

There are several particle tracking tools, or drift methodologies, specifically designed for integrating equations 1 - 4. Three tools are available in this framework: Ariane, OpenDrift and Modèle Lagrangien de Dispersion des Particules d'ordre n (MLDPn). The purpose of including several options is to determine how the choice of drift methodology might impact the result of the drift simulation. While each option aims to solve the same the equation, there are subtle differences in interpolation, regridding and land-particle interaction. Each of the three options is described in more details below.

It should be noted that many other drift methodologies and tools exist. These three were selected initially because they are used within the scientific community, including various research activities in the Government of Canada. Additional methodologies will be considered in future work.

2.2.1 Ariane

Ariane is a widely used Fortran tool for Lagrangian particle tracking (Blanke et al. 1997; Blanke et al. 1999; Blanke et al. 2001). Ariane is designed to work with three-dimensional ocean model output on the staggered Arakawa C-grid which is a common ocean model discretization for solving the equations of motion where the currents and tracers are on staggered grids. Ariane works by calculating the exact streamlines from a three-dimensional ocean velocity field. For stationary velocity fields, that is, velocity fields that are constant in time, streamlines are identical to particle trajectories. However, in non-stationary fields, that is, velocity fields that change over time, streamlines and particle trajectories diverge. As such, Ariane treats the velocity fields as stationary between ocean model output times. In addition, Ariane assumes velocity fields vary linearly between ocean model grid cells which preserves the divergence-free condition of the flow fields.

Ariane is widely used in water mass tracking and biological drift applications, but is not typically used in oil spill modelling or search and rescue applications. This is because it does not have the ability to include the influence of winds or other forces beyond ocean currents on particle motions nor does it account for the fate and behaviour of oil. Since Ariane predicts the streamlines of a velocity field, which satisfies no flow through coastal boundaries, no treatment of land-particle interaction is needed for particles where the land is taken from the ocean model grid.

At the time of writing this report, Ariane version 2.3.0 was used in this framework.

2.2.2 OpenDrift

OpenDrift is an open source Python package used to simulate drift trajectories in the marine environment (Dagestad et al. 2018). The package is used by the Norwegian Meteorological Institute to support oil spill response, search and rescue, and ship drift. Its modular design enables additional applications such as studies in larval dispersal and plastic tracking using a variety of ocean, atmosphere and wave model inputs from different grids and configurations.

In contrast to Ariane which calculates streamlines, OpenDrift applies time stepping algorithms such as forward Euler or Runge-Kutta to determine particle positions. As such, the accuracy of the OpenDrift trajectories depends on the integration time step, Δt, and the order of the time stepping algorithm. Smaller time steps and higher order methods are generally more accurate but also more computationally expensive. OpenDrift works well with ocean model output on any grid, particularly those with well defined projections such as polar stereographic or latitude-longitude, however, special treatment of the velocity fields is required for ocean velocities provided on the staggered Arakawa C-grid. In most cases, OpenDrift internally handles re-projecting and rotating vector data, however, some additions to OpenDrift were included for this project.

OpenDrift supports several options for land-particle interactions, such as permanent grounding, re-circulation, and no land effects. For the purposes of the framework presented in this report, particles that interact with land are moved to their previous position in the water. As such, they will continue to interact with land until the forces (wind, ocean, waves, or other) direct them away from the coast. Two options are available for defining land: either land is taken from ocean model grid or land is determined from a global coastline database provided by OpenDrift. For consistency with the ocean model solution, the former is recommended.

At the time of writing this report, OpenDrift version 1.10.7 was used within this framework with some customization to support the Arakawa C-grid from the Nucleus for European Modelling of the Ocean (NEMO) ocean model and atmospheric data on an irregular grid. In the case of Arakawa C-grid from NEMO output, the velocity vectors are rotated to the cardinal directions and then interpolated onto a regular grid before being used to solve the drift trajectories. Similarly, atmospheric data on an irregular grid is interpolated to a regular grid, however, the user must ensure that the wind vectors provided are already aligned with the cardinal directions. As with re-projecting data from other sources, these regridding operations are handled internally within the OpenDrift software. These modifications are available in a fork of the OpenDrift repository here:
`https://gitlab.com/dfo-drift-projection/dfo-opendrift`.

2.2.3 MLDPn

MLDPn is a particle tracking tool developed at Environment and Climate Change Canada (ECCC) to support transport and dispersion modelling in the atmosphere and marine environment (D'Amours et al. 2015). Oil spill modelling and tracking, including the fate and behaviour of oil, is available in MLDPn via the Canadian Oil Spill Modelling Suite (COSMoS; Marcotte et al. 2016). In addition to oil spill modelling, MLDPn can be used to support Leeway drift modelling, which is often used in search and rescue and vessel adrift applications (Allen 2005). The drift tool framework presented in this report uses MLDPn in a simplified fashion to numerically integrate equations 1 - 4. That is, Leeway and oil spill modelling are not currently available via MLDPn in this framework.

MLDPn handles input data from many different sources and grids by interpolating and re-projecting all required fields to a regular grid with a resolution defined by the user in a pre-processing step. In addition, a mask file which defines land points is generated from a large global coastline database. As a result, the definition of land in the drift simulation is not always consistent with the land used by the

ocean model. With respect to time-stepping, several options are available, including forward Euler and 4th-order Runge-Kutta for which users can specify the time step Δt as an input parameter.

At the time of writing this report, MLDPn version 5.0.1 was used as part of this framework.

2.3 Framework Modules

This framework provides three main modules. The purpose of each module is briefly described below:

1. **Drift Eval** - compare modelled drift trajectories with observed drift tracks.
2. **Drift Map** - describe the modelled flow characteristics using Lagrangian methods.
3. **Drift Correction Factor** - compare modelled velocities with observed drifter velocities.

Although each module serves a different purpose, they each follow a similar end-to-end process or workflow:

1. Read a configuration file which defines the data and parameters to be used;
2. Scan data directories and store metadata;
3. Perform computation or simulations as individual runs;
4. Apply post-processing to all outputs;
5. Plot and analyze the results.

Each of these steps are broken up into smaller parts to enable reproducibility, testing, and re-use of code. More details on each of the three modules are provided next, following some recommendations on the preparation of observed drifter data for the Drift Eval and Drift Correction Factor modules.

2.3.1 Recommendations for preparing observed drifter data

The following items should be considered when preparing drifter data for the purposes of applying this tool to compare with ocean model trajectories and velocities.

1. Quality control

   Drifter data should be quality controlled by flagging data entries that are not freely floating at sea. For example, data points on land, in an inter-tidal zone, trapped against cliffs, on a boat, etc. should be flagged as not freely floating (see Pawlowicz et al. 2019; Hourston et al. 2021). Bad GPS fixes or impossible times and coordinates should also be flagged as not freely floating at sea.

2. Data gaps

   Drifter tracks should be split into separate segments according to when the drifter is continuously at sea. In addition, trajectories with a large time gap should be split into multiple files. The recommended time gap is 6 hours, however, the underlying dynamics of the region might suggest consideration of a smaller time gap. In regions where currents are highly variable (e.g, tidally dominated areas) a smaller time gap of one or two hours should be considered.

3. Removal of flagged data

   Only data entries identified as freely floating at sea should be retained.

4. Temporal resolution

   It is recommended that the drifter data are resampled to a uniform output frequency. The resampling period is at the user's discretion and should be selected based on the original temporal resolution of the drifter data, the model's temporal resolution, and the dynamics of the region of interest. A good rule of thumb is to select a resampling period at the temporal resolution of the ocean model or less. One should avoid resampling to a period smaller than the original drifter data sampling period. Where velocities are estimated from the drifter data, a first-order forward difference method is applied, meaning that errors in this approximation are proportional to the temporal resolution of the data provided.

The Python package includes scripts suitable for addressing the last three items. The initial quality control step of identifying whether or not the drifter is at sea, however, is typically a manual process, especially when drifters are in near-shore areas where grounding probabilities are high (Pawlowicz et al. 2019). While the quality control of drifter data is not a focus of this report or framework, other projects within OPP have applied tools for this purpose (see Hourston et al. 2021).

2.3.2 Drift Eval

The Drift Eval module compares modelled drift trajectories to observed drifter trajectories over a time period of interest and under user-specified forcing conditions and simulation settings. It then produces a standardized set of outputs and evaluation metrics that are formatted in a consistent way regardless of the drift methodology used to generate the results. Plotting and analysis routines intake these standardized outputs to summarize and visualize the evaluation metrics. Here, we describe the procedure for generating and organizing the modelled drift outputs before they are processed for analysis and visualization. Examples of the available plotting and analysis results are shown in section 3.1.

To generate modelled and observed comparisons, multiple modelled trajectories are released along each observed drift track. For example, Figure 1 shows the model release positions and trajectories for a single drifter in an experiment forced with Coastal Ice Ocean Prediction System for the West Coast of Canada (CIOPS-W) ocean currents (Paquin et al. 2021b) and High Resolution Deterministic Prediction System (HRDPS) winds (Milbrandt et al. 2016). The release intervals, drift duration and time period of interest are parameters that are specified by the user and should be selected based on the application of interest (see section 2.3.2.1). For example, in regimes where the circulation pattern follows a steady mean direction and currents are not highly variable (e.g. boundary currents associated with large oceanic gyres), a long drift duration (e.g. 10 days) with daily releases might be appropriate. In contrast, in regions of highly variable or tidally-dominated currents, a shorter release interval and drift duration is recommended. The approach of releasing multiple modelled drifters per observed drifter has the disadvantage that scores for individual releases may be correlated, for example, during a large storm or event that might bias the surface currents in the model. However, given that modelled and observed drift tracks can separate rapidly with time a single release for each observed drifter is not representative of the model skill.

Initial positions of the modelled drifters are determined from the observed drifter trajectories by linearly interpolating the observed positions to the model release times. As such, large gaps in the observed time series can result in interpolation errors and uncertainty in the model initial positions. It is recommended that the user separates the observed drift tracks into multiple segments before including them in the evaluation when there are large temporal gaps in the time series. Furthermore, in the post-processing stages of this module, modelled drift predictions are interpolated to observed output times so a uniform output frequency among all drifters supports a standardized evaluation of the modelled drifters. Refer to section 2.3.1 for recommendations on preparing drifter data.

2.3.2.1 Recommendations for selecting release interval, drift duration, and time period

The following recommendations are intended to guide users in selecting the drifter release interval, drift duration, and time period over which the comparison is performed.

1. Release interval

   A good rule of thumb is to select a release interval equal to the model output period.

2. Drift duration

   When selecting the drift duration, the application supported by the evaluations should be considered. For example, for search and rescue or oil spill applications, a typical duration is 24 to 48 hours. For an evaluation of the general circulation in the open ocean or continental shelf, a duration of seven to ten days is appropriate. Furthermore, the typical length of the observed tracks is another factor to consider because comparisons will not be performed on track segments with lengths less than the drift duration.

3. Time period

   The time period, or start and end date of the comparison, largely depends on the availability of model and observational data. Users are encouraged to select a time period that covers a large portion of their data.

2.3.2.2 Evaluation metrics

During the post-processing stages of this module, several metrics for evaluating the accuracy of drift predictions are available and described below. Many of these metrics depend on the distance travelled by the drifter (l_n), the separation distance between the observed and modelled drifter (d_n), the observed drifter's displacement from its point of origin (D_n), and the distance between consecutive points in the observed track (δl_n). These quantities are illustrated in Figure 2.

Separation distance A practical and natural choice for defining an evaluation metric is the separation distance, D_n, between the observed drifter and the modelled drifter at any given point in time. Generally, a large separation distance indicates poor skill and a small separation distance indicates good skill. Yet, this metric poses challenges when analyzing many drifters that extend over a large geographical area or a long period of time. This metric is sensitive to the speed the drifter is travelling, that is, drifters that are travelling in an area where speeds are large are more likely to report higher separation distances. As such, when calculating averages across regions with variable currents, drifters in areas where currents are strongest can potentially skew the mean.

Molcard skill score Molcard et al. (2009) proposed a method to account for the drifter's speed by normalizing the separation distance by the displacement of the observed drifter from the origin. Using this strategy, the Molcard skill score, M_n is defined below:

$$M_n = \begin{cases} 1 - \frac{d_n}{D_n}, & \text{if } d_n < D_n \\ 0, & \text{if } d_n \geq D_n \end{cases} \tag{5}$$

A perfect agreement between the modelled and observed drifter position is realized when the separation distance is zero, in which case $M_n = 1$. When the separation distance is greater than the observed displacement from origin, the model is said to have no skill and $M_n = 0$ in which case the model performs no better than the last known position.

The Molcard skill score can be considered an instantaneous score. Normalization by the observed displacement from origin, D_n, poses some challenges in circumstances where drift trajectories are

elliptical or circular as might be observed in a tidally dominated region with a small background flow or areas where inertial currents are dominant. In this situation, D_n oscillates between near-zero and some maximum displacement every tidal or inertial cycle which also gives a cyclical pattern to the Molcard score.

Liu skill score Liu et al. (2011) proposed a cumulative skill score that takes into account the entire history of drift trajectory:

$$L_n = \begin{cases} 1 - \frac{s_n}{T}, & \text{if } s_n < T \\ 0, & \text{if } s_n \geq T \end{cases} \tag{6}$$

where T is a tolerance threshold and

$$s_n = \frac{\sum_{i=1}^{n} d_i}{\sum_{i=1}^{n} l_i}.$$

In this equation l_i is the distance the observed drifter travelled at time i,

$$l_i = \sum_{j=1}^{i} \delta l_j$$

As argued by Liu et al. (2011), a tolerance threshold of $T = 1$ is used in this report, meaning that the average separation distance should be less than the average distance travelled by the observed drifter in order for the model to have any meaningful skill.

Using this metric, a perfect drift prediction is realized when the separation distance is zero over the entire history for the track, in which case $L_n = 1$. The model is said to have no skill when the sum of the separation distances, d_i, is greater than the sum of the observed trajectory lengths, l_i. As a result, this score tends to weight early parts of the trajectory more heavily because $\sum_{i=1}^{n} l_i = n\delta l_1 + (n-1)\delta l_2 + (n-2)\delta l_3 + ... + \delta l_n$. A disadvantage of this score is that, given it is an integrated quantity, it is sensitive to the output frequency. As such, drifter trajectories should all be reporting at the same frequency when using this metric.

Sutherland skill score A final skill score is presented, which is also a cumulative score that accounts for the entire history of track and is formulated using a geometric argument involving areas constructed out of the distance metrics defined in Figure 2 (G. Sutherland 2019, personal communication). Two areas are considered: 1. $d_n \delta l_n$ (i.e., the product of the length of the observed track segment and the separation distance) and 2. $D_n \delta l_n$ (i.e., the product of the length of the observed track segment and the observed displacement from origin). A normalized cumulative skill score is constructed out of sum of these areas below:

$$S_n = \begin{cases} 1 - \frac{\sum_{i=1}^{n} d_i \delta l_i}{\sum_{i=1}^{n} D_i \delta l_i}, & \text{if } \sum_{i=1}^{n} d_i \delta l_i < \sum_{i=1}^{n} D_i \delta l_i \\ 0, & \text{if } \sum_{i=1}^{n} d_i \delta l_i \geq \sum_{i=1}^{n} D_i \delta l_i \end{cases} \tag{7}$$

A perfect skill is indicated when $S_n = 1$ and no skill when $S_n = 0$. As with the Liu score, S_n should be calculated using drifter data with a uniform output frequency.

Once these evaluation metrics are computed, the outputs are stored and saved in a separate netCDF file for each observed drifter. These files are then provided as inputs in the analysis routines associated with this module. The various analysis and plots provided by this module are described in section 3.1.

2.3.3 Drift Map

The Drift Map module works exclusively with model data to produce predicted drift trajectories over a region of interest. The purpose of this module is to describe the circulation patterns under the forcing conditions specified by the users. To accomplish this goal, the user provides the latitude and longitude coordinates of a rectangular region of interest and the number of particles to be released along the x (N_x) and y (N_y) coordinates. Then, a grid of N_x by N_y particles is initialized for each release time in the simulation. The number of releases is determined by the user-specified time period of interest and the release frequency, similar to the Drift Eval module.

During post-processing, metrics such as the distance travelled and displacement from origin for each drifter in the grid are computed and stored in netCDF files. In addition, the ratio between the displacement from origin and the distance travelled, which describes the degree to which the trajectory deviates from a straight line, is calculated and made available in the outputs. The results can then be summarized via specialized plots described in more detail in section 3.2.

It should be noted that the plots generated in this module might be sensitive to the initial distribution of particles. It is recommended that at least one particle is initialized in each model grid cell, however, over large areas, this approach might lead to particle densities that are difficult to interpret visually via maps of particle pathways. Future work will consider more robust and statistical metrics of particle motions and separations such as gridded diffusivity and Lagrangian Coherent Structures (see van Sebille et al. 2018).

2.3.4 Drift Correction Factor

The Drift Correction Factor module is the only module that does not produce modelled drift trajectories. Rather, it makes a direct comparison between observed drifter velocities and modelled ocean and atmosphere velocities. In doing so, it generates a time series of correction factors that would need to be applied to the modelled ocean currents or winds in order to produce a perfect drift prediction.

In the case where both winds and ocean currents are supplied, this module rearranges the following equation to solve for α (Sutherland et al. 2020):

$$\boldsymbol{u_d} = \boldsymbol{u_o} + \boldsymbol{\alpha u_{10}} \tag{8}$$

where $\boldsymbol{u_d}$ is the drifter velocity, $\boldsymbol{u_o}$ represents the ocean current acting on the drifter, $\boldsymbol{u_{10}}$ is the 10-metre atmospheric velocity and $\boldsymbol{\alpha}$ is a wind correction factor with along-wind and across-wind components. Variables in bold represent vector quantities.

In addition to the wind correction factor, an ocean correction factor is also evaluated by rearranging the following equation to solve for $\boldsymbol{\gamma}$:

$$\boldsymbol{u_d} = \boldsymbol{\gamma u_o} \tag{9}$$

In solving these equations, the drifter positions are resampled to an hourly frequency and the drifter zonal and meridional velocities are calculated using a first-order, forward difference method. Then, the ocean (and atmosphere, if applicable) zonal and meridional velocities are interpolated in space and time to the observed drifter data points. When solving for $\boldsymbol{\gamma}$ ($\boldsymbol{\alpha}$), the result is a vector time series where the real part is an along ocean current (wind) correction factor and the imaginary part is an across ocean current (wind) correction factor.

In addition to the correction factors, this module produces a few comparison metrics between the observed drifter and ocean model velocities. These metrics include time series of the 1) difference between the ocean model bearing and the drifter bearing, 2) the difference between the ocean model speed and the drifter speed, 3) the eastward and northward components of the ocean model and drifter velocity vector difference, and 4) the magnitude and bearing of the ocean model and drifter velocity vector difference. These metrics are available in the output files after the application of the

post-processing routines. Summary statistics such as the average speed and bearing of the drifters and ocean model, and correlation coefficients between the drifter and model speed and bearing are then readily computed during analysis and plotting.

Following Han et al. 2008, additional summary metrics include the velocity difference ratio (VDR) and the speed difference ratio (SDR) defined below:

$$VDR = \frac{\sum \|\boldsymbol{u_o} - \boldsymbol{u_d}\|^2}{\sum \|\boldsymbol{u_d}\|^2} \tag{10}$$

and

$$SDR = \frac{\sum \left(\|\boldsymbol{u_o}\| - \|\boldsymbol{u_d}\|\right)^2}{\sum \|\boldsymbol{u_d}\|^2}, \tag{11}$$

where $\|\boldsymbol{a}\| = \sqrt{a_1^2 + a_2^2}$ and a_1, a_2 are the Cartesian vector components of $\boldsymbol{a}$.

Examples of the summary tables and visualization of the outputs from this module are provided in section 3.3.

3 Examples and Applications

A demonstration of each of Drift Eval, Drift Map and Drift Correction Factor modules is provided in the following sections though a series of examples and figures. The figures are all generated during the analysis and plotting portion of each module.

3.1 Drift Eval

The Drift Eval module supports several different types of analyses such as analysis of a single experiment, comparisons between multiple experiments, and analysis divided into user-defined geographic regions. Each of these types of analyses produces many different plots of the observed and modelled drifter tracks and average skill scores both in space and time. The outputs are intended to provide a summary of the skill across all drifters but also provide detail on the skill of each individual drifter if requested by the user. A few examples are provided next.

3.1.1 Single experiment

First, this section demonstrates a selection of plots that are available when analyzing a single drift experiment. In this example, modelled drift trajectories forced by surface currents from CIOPS-W and $\alpha = 0.01$ with winds from HRDPS are compared with a set of drifters released by the Institute of Ocean Sciences (IOS) in the Northeast Pacific in 2016. The drifter type is the Surface Circulation Tracker (SCT) described in Hourston et al. 2021. These drifters have a drogue which extends to about 39 cm below the water line and a small communications receiver that extends above the water line. As such, these drifters are expected to experience minimal direct influence by the wind. The simulations presented in this example do not explicitly account for wave effects via a stokes drift velocity from a wave model. Modelled drift tracks were calculated using the OpenDrift methodology.

First, an overview of the observed drifter tracks and model releases are presented in Figure 3. The study period is January 1, 2016 to December 31, 2016. The modelled drifters were released every 6 hours and each modelled drifter was predicted for a duration of 48 hours. Any observed SCT drifters in the study period and in the CIOPS-W domain were selected for the comparison. A total of 103 observed drifters were considered in this experiment which resulted in 1729 model releases and individual model tracks. Most of the drifters were released in the Salish Sea which is the coastal body of water between Vancouver Island and the mainland. Some drifters were also released in Hecate Strait and Douglas Channel. For most drifters, properties such as the direction of the circulation are generally aligned

between the model and observations, however, there are some discrepancies. For example, the modelled drifters released to the west of the northern tip of Vancouver Island travel a different direction when compared with the observed drifter. In this area, wave effects (which are not included in this simulation) are likely more significant than in the more protected semi-enclosed Salish Sea. There are also noticeable differences in the observed and modelled speeds for the drifters released in Hecate Strait where the length of the modelled tracks are much shorter than observed.

A quantitative comparison between the model and observations is provided in summary plots of the separation distance and Molcard skill scores (see section 2.3.2.2) over the entire experiment (Figures 4 and 5). Scores for all drifter releases are binned by hour since release and then the average score and associated 25th and 75th percentiles for each hourly bin are plotted. In Figure 4, the average separation distance increases over time up to approximately 18 km after a 48 hour period. As typical for these types of comparisons, the modelled and observed tracks separate over time. There is a large degree of variability in the separation distance with an interquartile range of approximately 16 km at 48 hours.

In Figure 5, the average Molcard score ranges between 0.22 and 0.3 for the 48 hour duration, indicating that on average the model prediction is better than the last known position. Yet, at least 25% of the drifters do not perform better than the last known position, as indicated by the 25th percentile which is zero throughout the duration of the experiment. There is not a significant increase or decrease in the average Molcard score over this duration. Although not shown here, similar plots for the Liu skill score and Sutherland skill (see section 2.3.2.2) score can be produced. In addition, these line plots can be customized to show the standard deviation around the mean or bootstrapped 95% confidence intervals instead of the 25th and 75th percentiles, if desired.

Next, a summary of the skill scores by geographic area is provided in Figure 6 and Figure 7. In these plots, skills scores are grouped into hexagonal bins according to their model release position and the average score in each hexagon is computed and indicated by the colour mapping. We have presented the scores in this way because the initial release location is an important known quantity in many drift applications such as search and rescue and oil spill response. These two plots show average scores at 48 hours after the model release. Additional output times could be selected and plotted. The 48-hour average separation distance in Figure 6 highlights regions where the model-observation match is poor such as in the region to the west of the northern part of Vancouver Island where average separation distances are generally over 42 km. The poor match in this area is also obvious in Figure 3 where the model tracks are sometimes travelling in an entirely different direction than the observations. Finally, the 48 hour Molcard score (Figure 7) shows values near zero in this region. Note the relatively good agreement in the Strait of Juan de Fuca and the coastal current west of Washington State.

In addition to summary statistics over the entire dataset, this module can also produce plots of skill scores and tracks for each individual drifter in the dataset. An example is shown in Figure 8 where the average skill scores over each model release of a single drifter are shown. The skill scores are binned by hour since model release and then the average for each hourly bin is calculated and plotted. This particular drifter was released at the mouth of the Strait of Juan de Fuca and travelled westward where it circulated around an eddy at the mouth of Barkley Sound. The model mismatch in the eddy is apparent where modelled tracks deviate significantly from observations. With respect to skill scores, the average separation distance increases to nearly 22 km at the end of the 48 hour duration. The mean Molcard skill varies between 0.22 and 0.33 with a peak at around 22 hours. This score suggests the model is performing better than last known position for this drifter. The mean Liu score varies from 0.2 to 0.44 and increases over time.

Although not shown here, the module also produces summary tables of skill scores and other statistics such as the number of model releases, the number of observed drifters, and a list of the drifters used in the experiment. In addition, plots of persistence tracks, that is, a projection of the drifter position if the speed and direction at the time of release remained constant over the entire duration, can be produced.

3.1.2 Comparison experiment

In addition to analysis and plots for a single experiment, this module supports comparison across multiple experiments in order to explore the sensitivity of drift simulations to different modelling choices such as the wind drift factor, ocean model, atmospheric model, etc. In the following figures, example outputs and plots for comparisons between experiments are provided. As an extension to the single experiment presented in the previous section, which used CIOPS-W surface currents and $\alpha = 0.01$ with winds from HRDPS, two additional experiments are analyzed: an experiment with $\alpha = 0$ and an experiment with $\alpha = 0.02$. All experiments were run over the period of January 1, 2016 to December 31, 2016 using OpenDrift. Modelled drifters were released every 6 hours for a 48 hour duration and the same drifter dataset and models are used in all three experiments. In order to facilitate comparisons, the outputs of each experiment are subset to include only the drifter segments that intersect over all experiments.

A first comparison plot is provided in Figure 9 where the average separation distance as a function of time since model release is shown for each experiment. At the end of the 48 hour simulation period, the experiment with CIOPS-W ocean currents and $\alpha = 0.01$ with winds from HRDPS exhibits the smallest average separation distance of 17.8 km. Comparatively, the experiments with $\alpha = 0$ and $\alpha = 0.02$ have average separation distances of 19.6 km and 18.4 km, respectively. Similar plots for the Molcard skill score, Liu skill score and Sutherland skill score could be produced, as required.

In addition to these lines plots, this module also provides mapped comparisons by plotting the average difference in separation distance at a specified time. For example, Figure 10 shows the average difference in the separation distance between the experiment with $\alpha = 0.01$ and $\alpha = 0$ at 48 hours after model release. The skill scores are grouped spatially into hexagonal bins based on the initial release location and then the average value is calculated and plotted. In this example, the blue regions indicate that the experiment with $\alpha = 0.01$ has smaller separation distances. In contrast, red areas represent regions where the $\alpha = 0.01$ experiment has larger separation distances. Notably, the $\alpha = 0.01$ case leads to a general improvement (that is, lower separation distances) for the drifters released west of Vancouver Island.

The difference in separation distance is also available as a function of time in Figure 11 which shows the difference between the experiments with $\alpha = 0.01$ and $\alpha = 0$. The difference in separation distance is grouped into hourly bins and then the average for each hour is calculated and plotted for each individual drifter in the coloured lines. The solid black line is the average over all drifters in the experiment. This plot demonstrates that the experiment with $\alpha = 0.01$ has, on average, smaller separation distances, indicating a better match with observations. Note that the Molcard, Liu and Sutherland scores are not available in difference plots. To produce a difference plot, the user is expected to define a reference experiment. All differences are computed relative to the reference experiment.

3.1.3 Regional comparison

Another feature of the Drift Eval analysis is the ability to separate the analysis into individual regions. In this approach, the user provides an input file which describes the coordinates of the regions for the analysis. Modelled drifters are then grouped into each region based on their initial release position. Then, statistics and skill scores are calculated and plotted for each region.

To demonstrate a few of the plots available in a regional comparison, the three experiments discussed in the previous section are used. These experiments include CIOPS-W surface currents and winds from HRDPS with $\alpha = 0$, $\alpha = 0.01$, and $\alpha = 0.02$. In fact, the same modelled drift data files are used as inputs into the analysis routines, however, an additional argument that points to a file describing the regional coordinates triggers the application of a regional analysis.

First, a visualization of the user-defined regions and the model release positions is provided in Figure 12. Eight distinct regions are defined: Juan de Fuca West (JdFW), Juan de Fuca East (JdFE), Gulf Islands (GulfIsl), Haro Strait (Haro), Straight of Georgia North (SoGN), Straight of Georgia South

(SoGS), Vancouver Harbour (VH), and Howe Sound (Howe). For each experiment, the analysis is performed over each of these regions in addition to the polygon resulting from the combination of all the regions. Finally, the analysis is performed over the entire dataset, including the drifters released outside of any of the regions. A summary of the average separation distance at 48 hours after release is provided in Table 1. Similar tables for the other skill scores, like Molcard, Liu, and Sutherland, can be produced but are not provided in this report. The table confirms that the $\alpha = 0.01$ case generally has the smallest separation distances in SoGS, Howe, Haro, and JdFE. The $\alpha = 0$ experiment has the smallest separation distances in VH and JdFW and the $\alpha = 0.02$ experiment has the smallest separation distances in GulfIsl and SoGN.

Next, a demonstration of some of the plots available in each region is provided. Only the SoGN region is shown, although similar plots are produced for all regions. The observed drifters available in the SoGN region are shown in Figure 13. In this region, a total of eight observed drifters are available which results in 128 model releases. Similar statistics are available for the other regions.

A comparison of the separation distance as a function of time in SoGN is provided in Figure 14 for each of the three experiments. At the end of the 48 hour duration, the $\alpha = 0.02$ experiment exhibits the smallest separation distances, however, this plot demonstrates that the separation distance across these three experiments do not differ substantially in this region.

Finally, plots of mapped skill scores are also available in a regional comparison analysis. An example is provided for the 48-hour average Molcard skill score in Figure 15 in the SoGN region for the experiment with $\alpha = 0.01$. This figure demonstrates that the complex drift trajectories in the southern part of this region (Figure 13) are not well represented. The Molcard skill score is close to zero in a large portion of this part of the domain.

Although not shown here, there are many additional plots available for each region. These additional plots include difference plots such as those shown in Figures 10 and 11. In addition, the user can request plots of modelled and observed drifters on the same map like in Figure 3, and plots of individual drifters and their associated skill scores like in Figure 8. The regional sub-division allows for more refinement of the analysis to explore the impacts of different dynamical processes on the drift skill. Finally, a regional analysis can also be applied to a single experiment.

3.2 Drift Map

An example of the outputs available with the Drift Map module is provided next. In this example, a grid of 25 x 25 particles was initialized in a region over the Northwest Atlantic and forced by Global Ice Ocean Prediction System (GIOPS) ocean currents at 15 m depth using Ariane. The particles were released on June 8, 2016 and were simulated for a duration of 10 days.

A map of the trajectories is shown in Figure 16 where large displacements are observed for particles initialized along the northern edge of the Grand Banks due to the relatively fast moving Labrador Current. Eddies from the Gulf Stream are also apparent in the map where some particles are following large, circular pathways in the region south of Flemish Cap. In addition to snapshots of the trajectories, the plotting routines in this module produce an animation of the trajectories for each modelled release. Although not shown here, this example also produced trajectories initialized on June 9 and 10, 2016. The release frequency and start/end dates are defined in a configuration file.

In addition to maps of the trajectories, some statistics regarding the maximum displacement from origin and distance travelled are provided in Figure 17. Over the 10-day period, more than half of the particles travelled a maximum distance of less than 100 km. The average maximum distance travelled was 154 km with standard deviation 142 km. The mean is skewed by the small number of particles that travelled large distances of over 300 km. The displacement histogram is also skewed with more than half of particles displaced at maximum 100 km from their initial position. These histograms are sensitive to the initial distribution of particles. In this example, a large number of particles were initialized in the relatively quiescent regions like the Grand Banks.

Finally, a histogram of the ratio between the displacement from origin and the total distance travelled is shown in Figure 18. This metric describes the degree to which a trajectory deviates from a straight line, where a value of one indicates the trajectory is a straight line and values less than one indicate curved and meandering trajectories. In this example, the average value of this ratio is 0.69 and the distribution is skewed to the right indicating that most trajectories are following a relatively linear (as opposed to circular) pathway.

3.3 Drift Correction Factor

A demonstration of the Drift Correction Factor module and some of its output is provided next. This example uses drifter data collected during a large field campaign called the Tracer Release Experiment (TReX) which took place in the St. Lawrence Estuary in September 2020 and 2021 (Pawlowicz et al. 2021). During this experiment, over 200 drifters of varying shapes and configurations where deployed (Pawlowicz et al. 2024). A subset of these drifters, including 20 Osker surface floats (Xeos Technologies Inc., Canada) released in September 2020 (Figure 19), is used for this demonstration. In addition, ocean and wind forcing is provided by hourly surface currents from the Coastal Ice Ocean Prediction System for the East Coast of Canada (CIOPS-E) ocean model (Paquin et al. 2021a) and 10-metre winds from the HRDPS atmospheric model (Milbrandt et al. 2016), both of which were developed at ECCC.

The analysis component of this module provides several figures and comparisons for each individual drifter. Examples for one of the drifters is available in Figures 20 to 22. In Figure 20, a plot of the drifter's trajectory is shown on the map. As well, the time series of the drifter's eastward and northward velocity components and speed is displayed. Included are the equivalent variables from the ocean model and atmosphere model, interpolated to the drifter track in both space and time. The semi-diurnal tidal signal is apparent in both the drifter and ocean model. In addition, a strong northeasterly wind event on September 23 is observed in the wind time series. This strong wind event appears to have influenced the drifter's northward velocity and speed where spikes in those time series are evident.

Next, following Sutherland et al. 2020, an example of the distribution of $\boldsymbol{\alpha}$ for a single drifter is shown in Figure 21 as a two-dimensional histogram of the real and imaginary components. The histogram shows that there is a large amount of spread in the both the real and imaginary parts of $\boldsymbol{\alpha}$ with values ranging from ± 0.3 and standard deviations of 0.053 for Re($\boldsymbol{\alpha}$) and 0.073 for Im($\boldsymbol{\alpha}$). The mean value for Re($\boldsymbol{\alpha}$) is approximately 0.017 and the mean value for Im($\boldsymbol{\alpha}$) is near zero. As discussed in Sutherland et al. 2020, a time series or spectral analysis of $\boldsymbol{\alpha}$ can prove useful for identifying periodicity in $\boldsymbol{\alpha}$ which might indicate an underlying mismatch between the model currents and observations for certain frequencies of motion. That type of analysis is not currently available in this package.

The rotary spectra for the drifter and ocean model velocity vectors are shown in Figure 22. Both the model and drifter velocities demonstrate a peak at the semi-diurnal tidal frequencies in both the clockwise and counterclockwise rotations. At higher frequencies, there is a mismatch between the model and drifter, with the model spectra nearly an order of magnitude smaller than the drifter. Note that the rotary spectra were calculated over the entire time series of the drifter track and no effort was made to divide the track up into shorter segments to account for spatially varying contributions to the spectra. In this plot, the rotary spectra were calculated using a multitaper method (Lees et al. 1995; Lilly 2022) in order to smooth the variance in the spectral estimate. The degree of smoothing is controlled by a parameter called the time-bandwidth product (P) where a higher value of P results in more smoothing. In this example, $P = 4$.

In addition to analysis performed on individual drifters, this module offers summary comparisons over the entire drifter dataset. As an example, Figure 23 shows the average difference between the ocean model speed and the drifter speed along the drifter tracks shown in Figure 19. Speed differences are grouped into hexagonal cells and the average speed difference is computed across all data points in each cell. The number of data points contributing to each cell is shown in Figure 24. In Figure 23, areas coloured blue show where the ocean model currents are on average slower than the drifter and red areas

show where the ocean model currents are on average faster than the drifter. It should be noted that wind can directly act on the observed drifters, and in turn, partially explain discrepancies between the ocean model and drifter speeds.

Next, a two-dimensional histogram comparing the drifter and observed velocity components is shown in Figure 25. In this case, the ocean model tends to underestimate the eastward velocity although there is a great deal of spread in the distribution. The distribution of the northward velocities also indicates the model is slightly underestimating the northward currents. A significant part of this distribution is in the second quadrant which suggests that the model, at times, exhibits southward velocities when the observed drifter is directed to the north. Again, the influence of wind on the observed drifters is not accounted for in this comparison.

Finally, a table summarizing several metrics for each drifter in addition to the entire dataset is provided by this module and shown in Table 2. Notably, the metrics involving bearing such as the mean bearing difference (Mean θ_D) and the correlation between the ocean model and drifter bearing ($r_{\boldsymbol{u_o u_d}\theta}$) show relatively poor skill. The mismatch in bearing is not surprising given the discrepancies in northward velocities noted in Figure 25.

4 Future Work

Comparisons between modelled and observed drift trajectories are complex. A number of improvements to this framework are being considered as future work. Some of these improvements include:

1. Accounting for uncertainty associated with drift predictions by releasing a large number of particles with random walks to represent diffusive and sub-grid scale processes.
2. Inclusion of stokes drift velocities as an additional input in Drift Correction Factor calculations.
3. Enhanced analysis of the wind effect in Drift Correction Factor post-processing and plotting.
4. Improved integration between Drift Correction Factor and Drift Eval to explore sensitivity of wind coefficients on evaluation metrics.
5. Exploration of new techniques, such as machine learning, in the selection of optimal wind coefficients.
6. Explore the impact of land-particle interaction and land definition in drift prediction solutions.
7. Improve code efficiency and provide support for parallelized computations.
8. Expand ability for user to customize figures and plot settings such as font size.
9. Explore additional evaluation metrics such as the Phillipson cross over time (Phillipson et al. 2018).
10. Expand analysis provided by the Drift Map module by considering gridded diffusivity and Lagrangian coherent structures.
11. Include support for unstructured grid ocean models.

5 Code Availability

The code for this framework is publicly available in a GitLab repository: `https://gitlab.com/dfo-drift-projection/drift-workflow-tool/`. The configuration files for the analysis examples discussed in this report are available in the repository. Further documentation on how to use the framework is available on the repository wiki. At the time of writing this report, version 6.2 was used.

Modifications to OpenDrift are available in a forked repository here: `https://gitlab.com/dfo-drift-projection/dfo-opendrift`. At the time of writing the `update-opendrift-1.10.7` branch was used.

6 Acknowledgments

A number of individuals and groups were involved in supporting this project. First, we'd like to thank Clyde Clements, Samuel Babalola, and Hauke Blanken for early contributions to the code development. Fraser Davidson, Guoqi Han, Greg Smith and Graig Sutherland provided meaningful feedback on the scientific approaches, methods and evaluation techniques to consider.

Thank you to the Drift Prediction and Near-Shore port modelling team, including Michael Dunphy, Rachel Horwitz, Stephanne Taylor, Hauke Blanken, Maxim Krassovski, Adam Drozdowski, and Simon St. Onge-Drouin for feedback and testing. In addition, Roy Hourston, Doug Schillinger, Justine Mcmillan and Grace Watts provided support for the quality control of drifter data. Patricia Pernica provided support on project oversight and reporting.

Support for MLDPn documentation and compilation was provided by Guillaume Marcotte, Éric Legault-Ouellet and Zhimin Ma. Jean-Philippe Paquin and François Roy provided ocean model data and Corinne Bourgault-Brunelle, Hui Shen, and Yvonnick Le Clainche assisted with organizing and de-archiving ocean and atmospheric model data.

Finally, we'd like to thank two reviewers, Yuehua Lin and Andry Ratsimandresy, for constructive comments and improvements to the report.

References

Abascal, Ana J, Sonia Castanedo, Fernando J Mendez, Raul Medina, and Inigo J Losada. 2009. Calibration of a Lagrangian transport model using drifting buoys deployed during the Prestige oil spill. Journal of Coastal Research **25**(1): 80–90.

Allen, Arthur A. 2005. Leeway divergence. US Coast Guard Research and Development Center.

Blanke, Bruno, Michel Arhan, Gurvan Madec, and Sophie Roche. 1999. Warm water paths in the equatorial Atlantic as diagnosed with a general circulation model. Journal of Physical Oceanography **29**(11): 2753–2768.

Blanke, Bruno and Stéphane Raynaud. 1997. Kinematics of the Pacific equatorial undercurrent: An Eulerian and Lagrangian approach from GCM results. Journal of Physical Oceanography **27**(6): 1038–1053.

Blanke, Bruno, Sabrina Speich, Gurvan Madec, and Kristofer Döös. 2001. A global diagnostic of interocean mass transfers. Journal of Physical Oceanography **31**(6): 1623–1632.

Breivik, Øyvind, Arthur A Allen, Christophe Maisondieu, Jens-Christian Roth, and Bertrand Forest. 2012. The leeway of shipping containers at different immersion levels. Ocean Dynamics **62**: 741–752.

D'Amours, Réal, Alain Malo, Thomas Flesch, John Wilson, Jean-Philippe Gauthier, and René Servranckx. 2015. The Canadian Meteorological Centre's atmospheric transport and dispersion modelling suite. Atmosphere-Ocean **53**(2): 176–199.

Dagestad, Knut-Frode, Johannes Röhrs, Øyvind Breivik, and Bjørn Ådlandsvik. 2018. OpenDrift v1. 0: a generic framework for trajectory modelling. Geoscientific Model Development **11**(4): 1405–1420.

Han, Guoqi, Zhaoshi Lu, Zeliang Wang, James Helbig, Nancy Chen, and Brad De Young. 2008. Seasonal variability of the Labrador Current and shelf circulation off Newfoundland. Journal of Geophysical Research: Oceans **113**(C10).

Hourston, Roy A S, Pauline S Martens, Tamás Juhász, Stephen J Page, and Hauke Blanken. 2021. *Surface ocean circulation tracking drifter data from the Northeastern Pacific and Western Arctic Oceans, 2014–2020*. Canadian Data Report of Hydrography and Ocean Sciences 215: p. 36.

Lees, Jonathan M and Jeffrey Park. 1995. Multiple-taper spectral analysis: A stand-alone C-subroutine. Computers & Geosciences **21**(2): 199–236.

Lilly, Jonathan M. 2022. *Ocean/Atmosphere Time Series Analysis*. Version 0.21. DOI: 10.5281/zenodo.5986397. URL: https://doi.org/10.5281/zenodo.5986397.

Lin, Yuehua, Michael Dunphy, Maxim Krassovski, Hauke Blanken, and Roy Hourston. 2022. *Preliminary Development of a Relocatable Ocean Model System for the West Coast of Canada: A Summary of OPP FA5 Modeling*. Canadian Technical Report of Hydrography and Ocean Sciences 343: p. 25.

Liu, Yonggang and Robert H Weisberg. 2011. Evaluation of trajectory modeling in different dynamic regions using normalized cumulative Lagrangian separation. Journal of Geophysical Research: Oceans **116**(C9).

Marcotte, G, P Bourgouin, G Mercier, JP Gauthier, P Pellerin, G Smith, and CW Brown. 2016. Canadian oil spill modelling suite: An overview. In: *39th AMOP technical seminar on environmental contamination and response*: pp. 1026–1034.

Milbrandt, Jason A, Stéphane Bélair, Manon Faucher, Marcel Vallée, Marco L Carrera, and Anna Glazer. 2016. The pan-Canadian high resolution (2.5 km) deterministic prediction system. Weather and Forecasting **31**(6): 1791–1816.

Molcard, A, PM Poulain, Philippe Forget, A Griffa, Yves Barbin, Joel Gaggelli, JC De Maistre, and M Rixen. 2009. Comparison between VHF radar observations and data from drifter clusters in the Gulf of La Spezia (Mediterranean Sea). Journal of Marine Systems **78**: S79–S89.

Nudds, Shannon, Youyu Lu, Simon Higginson, Susan P Haigh, Jean-Philippe Paquin, Mitchell O'Flaherty-Sproul, Stephanne Taylor, Hauke Blanken, Guillaume Marcotte, Gregory C Smith, et al. 2020. Evaluation of structured and unstructured models for application in operational ocean forecasting in nearshore waters. Journal of Marine Science and Engineering **8**(7): 484.

Paquin, Jean-Philippe, Youyu Lu, Stephanne Taylor, Hauke Blanken, Guillaume Marcotte, Xianmin Hu, Li Zhai, Simon Higginson, Shannon Nudds, Jérôme Chanut, et al. 2020. High-resolution modelling of a coastal harbour in the presence of strong tides and significant river runoff. Ocean Dynamics **70**: 365–385.

Paquin, Jean-Philippe et al. 2021a. *Coastal ice ocean prediction system for the East Coast of Canada (CIOPS-E): Update from version 1.5.0 to 2.0.0*. Canadian Centre for Meteorological and Environmental Prediction Technical Note. Environment and Cliamte Change Canada: p. 33.

Paquin, Jean-Philippe et al. 2021b. *Coastal ice ocean prediction system for the West Coast of Canada (CIOPS-W): Update from version 1.5.0 to 2.0.0.* Canadian Centre for Meteorological and Environmental Prediction Technical Note. Environment and Cliamte Change Canada: p. 42.

Pawlowicz, Rich, Cedric Chavanne, Dany Dumont, Roy Hourston, Douglas Schillinger, and Nancy Soontiens. 2021. *TReX Surface Dye Release Phase 1 Drifter Dataset*. DOI: http://dx.doi.org/10.14288/1.0398295. URL: https://open.library.ubc.ca/collections/researchdata/items/1.0398295.

Pawlowicz, Rich, Cédric Chavanne, and Dany Dumont. 2024. The Water-Following Performance of Various Lagrangian Surface Drifters Measured in a Dye Release Experiment. Journal of Atmospheric and Oceanic Technology **41**(1): 45–63.

Pawlowicz, Rich, Charles Hannah, and Andy Rosenberger. 2019. Lagrangian observations of estuarine residence times, dispersion, and trapping in the Salish Sea. Estuarine, Coastal and Shelf Science **225**(March): 106246. ISSN: 02727714. DOI: 10.1016/j.ecss.2019.106246.

Phillipson, LM and R Toumi. 2018. The crossover time as an evaluation of ocean models against persistence. Geophysical Research Letters **45**(1): 250–257.

Sutherland, Graig, Nancy Soontiens, Fraser Davidson, Gregory C Smith, Natacha Bernier, Hauke Blanken, Douglas Schillinger, Guillaume Marcotte, Johannes Röhrs, Knut-Frode Dagestad, et al. 2020. Evaluating the leeway coefficient of ocean drifters using operational marine environmental prediction systems. Journal of Atmospheric and Oceanic Technology **37**(11): 1943–1954.

Ullman, David S, James O'Donnell, Josh Kohut, Todd Fake, and Arthur Allen. 2006. Trajectory prediction using HF radar surface currents: Monte Carlo simulations of prediction uncertainties. Journal of Geophysical Research: Oceans **111**(C12).

van den Bremer, Ton S and Øyvind Breivik. 2018. Stokes drift. Philosophical Transactions of the Royal Society A: Mathematical, Physical and Engineering Sciences **376**(2111): 20170104.

van Sebille, Erik, Stephen M Griffies, Ryan Abernathey, Thomas P Adams, Pavel Berloff, Arne Biastoch, Bruno Blanke, Eric P Chassignet, Yu Cheng, Colin J Cotter, et al. 2018. Lagrangian ocean analysis: Fundamentals and practices. Ocean modelling **121**: 49–75.

Tables

Table 1: Average separation distance (m) at $t = 48$ hr for three experiments with varying wind factors as indicated by α. Average scores are grouped by regions defined in Figure 12.

	$\alpha = 0$	$\alpha = 0.01$	$\alpha = 0.02$
SoGS	21800	21134	24248
SoGN	23973	23248	22466
Howe	7938	7882	10508
VH	16004	17036	17888
GulfIsl	20368	21059	19443
Haro	31558	26227	27149
JdFE	19334	18968	19012
JdFW	13641	15500	18013
All Polygons	18394	18705	19869
Entire dataset	19619	17773	18393

Table 2: Comparison metrics produced by the Drift Correction Factor module. N is the number of data points accounted for in the calculation of statistics in each row. $\boldsymbol{u_d}$ and $\boldsymbol{u_o}$ are the drifter and ocean velocity vectors. The magnitude and bearing of vectors are represented by $\|\|$ and θ. r represents a correlation coefficient between the variables listed in each column (e.g. r $\boldsymbol{u_o u_d}$ east means the correlation coefficient between the eastward vector components of $\boldsymbol{u_o}$ and $\boldsymbol{u_d}$). SDR and VDR are the speed difference ratio and the velocity different ratio. $\boldsymbol{vvd} = \boldsymbol{u_o} - \boldsymbol{u_d}$ is velocity vector difference. θ_D is the difference in model and drifter bearing.

Drifter ID	N	Mean $\|\boldsymbol{u_d}\|$ (m/s)	STD $\|\boldsymbol{u_d}\|$ (m/s)	Mean $\|\boldsymbol{u_o}\|$ (m/s)	STD $\|\boldsymbol{u_o}\|$ (m/s)	r $\frac{\|\boldsymbol{u_o}\|}{\|\boldsymbol{u_d}\|}$	SDR	VDR	r $\boldsymbol{u_o u_d}$	r $\boldsymbol{u_o u_d}$ north	r $\boldsymbol{u_o u_d}$ east	Mean $\|\boldsymbol{vvd}\|$ (m/s)	STD $\|\boldsymbol{vvd}\|$ (m/s)	Mean θ_D (deg)	STD θ_D (deg)	r $\boldsymbol{u_o u_d}$ θ
1001300434064148020	382	0.44	0.33	0.39	0.27	0.46	0.33	0.65	0.62	0.49	0.63	0.39	0.22	57.88	49.24	0.35
1002300434064049950	382	0.46	0.29	0.38	0.23	0.51	0.26	0.56	0.64	0.49	0.56	0.35	0.21	46.27	42.88	0.41
1003300434064142020	382	0.47	0.24	0.40	0.23	0.37	0.27	0.68	0.57	0.37	0.56	0.39	0.19	54.85	48.28	0.25
1004300434064046670	342	0.48	0.25	0.37	0.25	0.51	0.25	0.74	0.52	0.28	0.58	0.41	0.22	67.65	58.77	0.23
1005300434064149010	319	0.44	0.22	0.33	0.21	0.38	0.28	0.86	0.43	0.42	0.41	0.40	0.22	70.43	55.43	0.17
1006300434064044960	382	0.46	0.26	0.43	0.25	0.37	0.30	0.70	0.58	0.41	0.55	0.40	0.18	54.91	50.07	0.31
1007300434064043660	382	0.47	0.31	0.37	0.24	0.51	0.27	0.62	0.64	0.47	0.64	0.40	0.20	58.08	50.20	0.22
1008300434064047660	382	0.45	0.26	0.41	0.23	0.35	0.30	0.79	0.53	0.33	0.53	0.41	0.21	63.50	54.32	0.17
1009300434064728070	382	0.47	0.25	0.33	0.23	0.48	0.28	0.64	0.58	0.37	0.61	0.38	0.20	58.27	48.59	0.30
1010300434064046920	341	0.44	0.27	0.44	0.20	0.39	0.27	0.61	0.63	0.67	0.56	0.36	0.19	43.75	43.13	0.26
890300434063390330	375	0.47	0.31	0.35	0.26	0.46	0.33	0.76	0.50	0.36	0.49	0.42	0.26	60.16	48.36	0.22
948300434064424470	372	0.45	0.30	0.37	0.23	0.24	0.40	0.98	0.37	0.20	0.36	0.47	0.26	71.45	51.07	0.20
949300434064329300	375	0.37	0.26	0.41	0.29	0.18	0.60	1.28	0.30	0.16	0.31	0.45	0.24	65.40	51.92	0.22
950300434064422480	373	0.47	0.31	0.34	0.25	0.46	0.32	0.74	0.51	0.38	0.51	0.41	0.24	61.82	48.03	0.21
951300434064325310	366	0.46	0.28	0.34	0.23	0.14	0.45	0.92	0.35	0.30	0.33	0.44	0.25	62.05	48.30	0.31
952300434064323300	366	0.44	0.29	0.34	0.22	0.26	0.40	0.87	0.48	0.24	0.51	0.42	0.26	63.28	52.70	0.27
953300434064420440	254	0.53	0.34	0.41	0.25	0.30	0.36	0.84	0.41	0.35	0.34	0.52	0.25	66.57	48.89	0.17
954300434064323280	375	0.47	0.30	0.37	0.23	0.34	0.34	0.78	0.50	0.41	0.48	0.45	0.22	64.49	48.04	0.24
955300434064320290	331	0.46	0.26	0.26	0.19	0.45	0.35	0.67	0.58	0.55	0.55	0.37	0.23	59.72	49.15	0.26
956300434064324300	380	0.47	0.29	0.35	0.24	0.50	0.28	0.65	0.61	0.37	0.69	0.40	0.20	61.14	49.48	0.34
entire dataset	7243	0.46	0.28	0.37	0.24	0.37	0.33	0.76	0.52	0.37	0.51	0.41	0.23	60.42	50.38	0.25

Figures

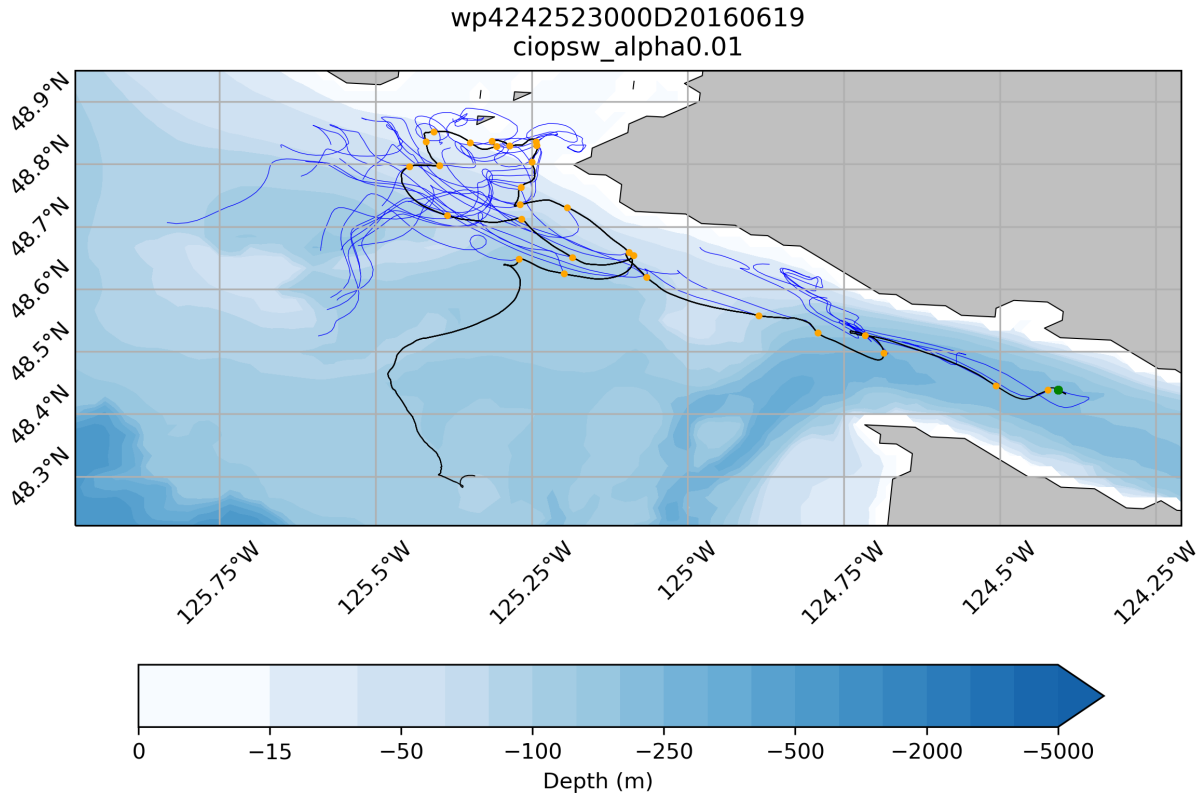

Figure 1: An example of the model initial positions (orange dots) and model drift trajectories (blue lines) for a single observed drift track (black line). The green dot is the starting position of the observed drift track which was released in June 2016. Land as defined by the ocean model land mask is shown in gray. Modelled drifters were released every six hours for a duration of 48 hours. The CIOPS-W ocean model surface currents were used along with winds from the HRDPS atmospheric model with $\alpha = 0.01$. In the title, wp4242523000D20160619 represents the drifter ID and ciopsw_alpha0.01 is a user defined identifier for the experiment.

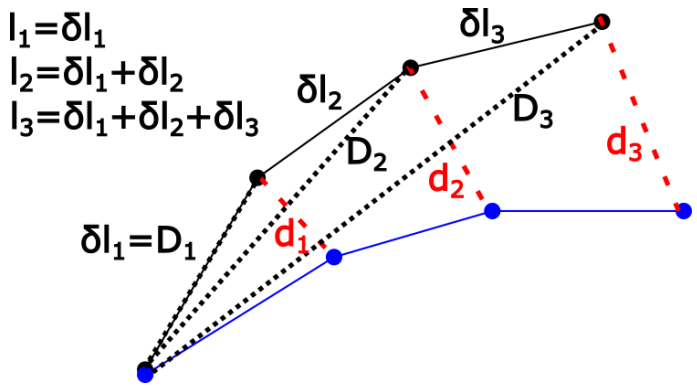

Figure 2: Distance definitions for a pair of observed (black) and modelled (blue) drifters. $l_n = \delta l_1 + \delta l_2 + ... + \delta l_n$ is the distance the observed drifter travelled at time n. d_n is the separation distance between the observed and modelled drifter at time n. D_n is the observed drifter's displacement from origin at time n. In this illustration, $n = 1, 2,$ or 3.

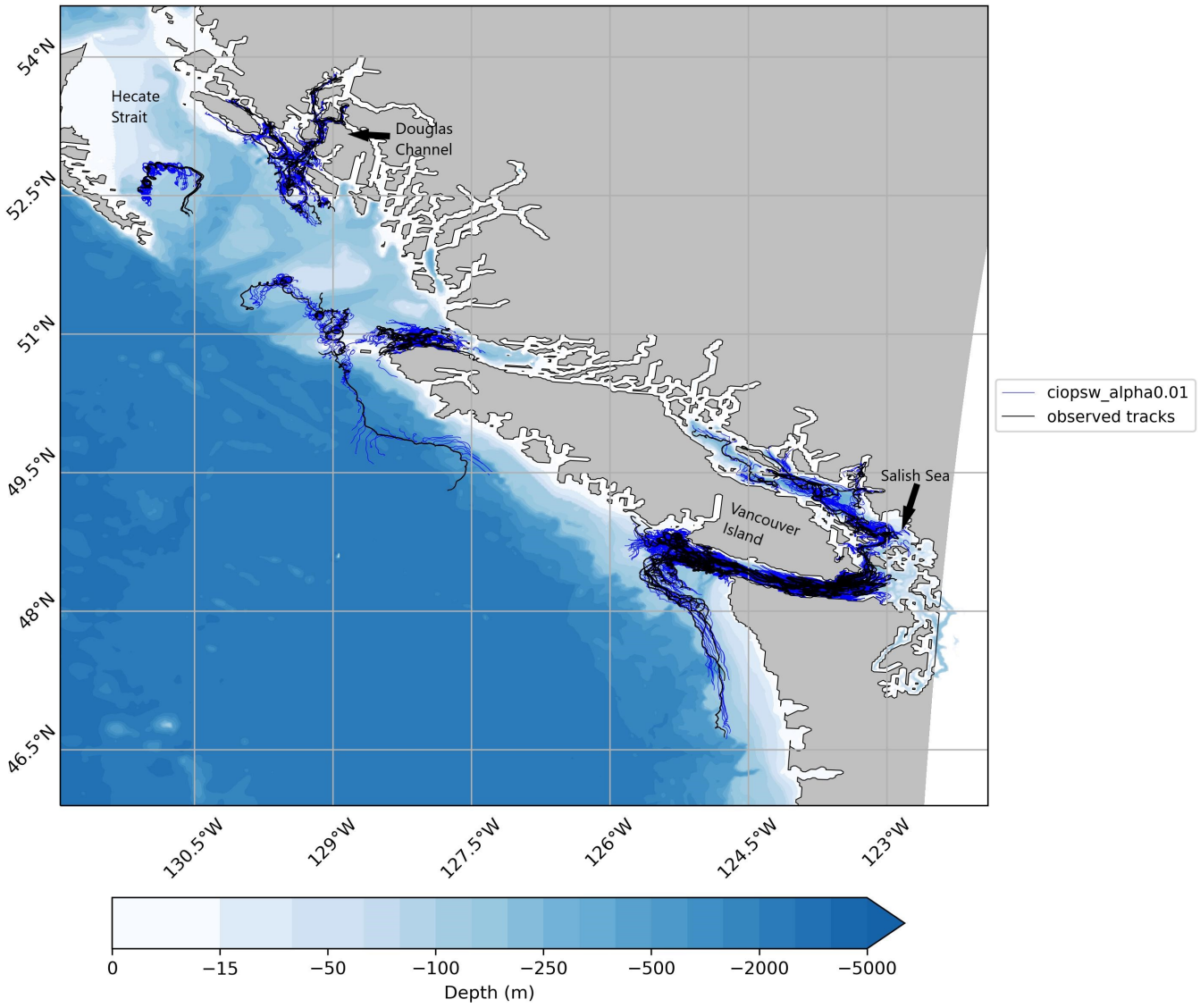

Figure 3: Observed (black) and modelled (blue) trajectories for a set of drifters released in the Northeast Pacific and Salish Sea in 2016. The modelled trajectories were forced with surface currents from the CIOPS-W model and winds from the HRDPS atmospheric model with $\alpha = 0.01$. Locations were manually added to the plot in a separate program.

.

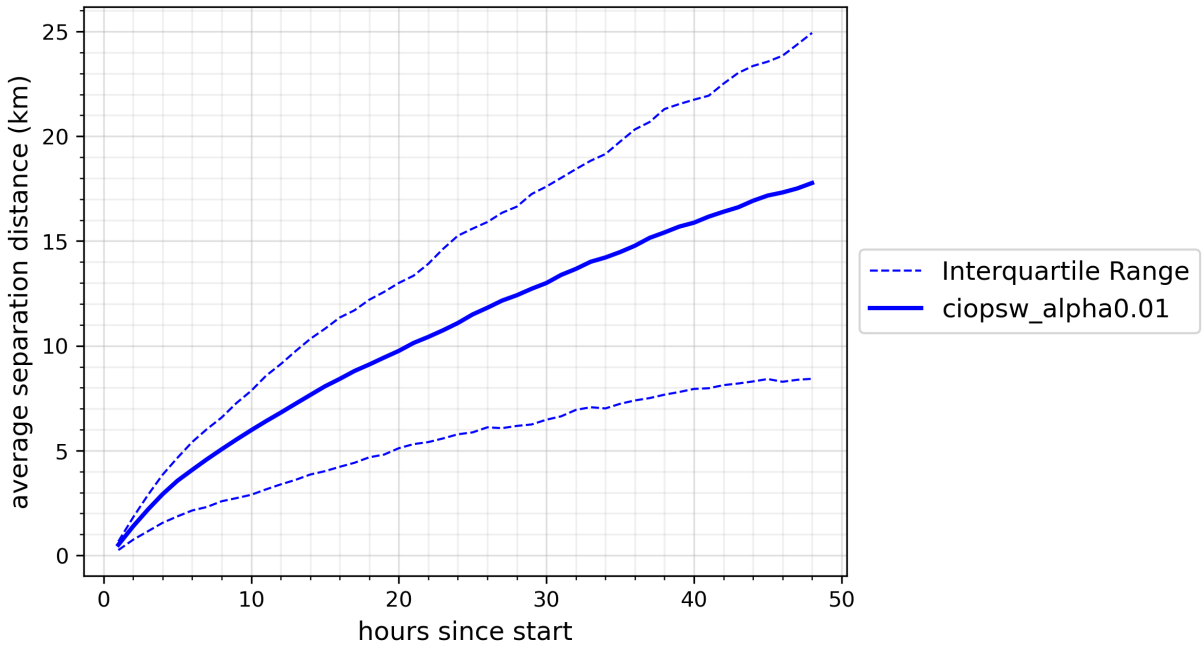

Figure 4: Average separation distance (solid line) as a function of time since modelled drifter was released for all tracks shown in Figure 3. The dashed lines represent the 25th and 75th percentiles of the distribution.

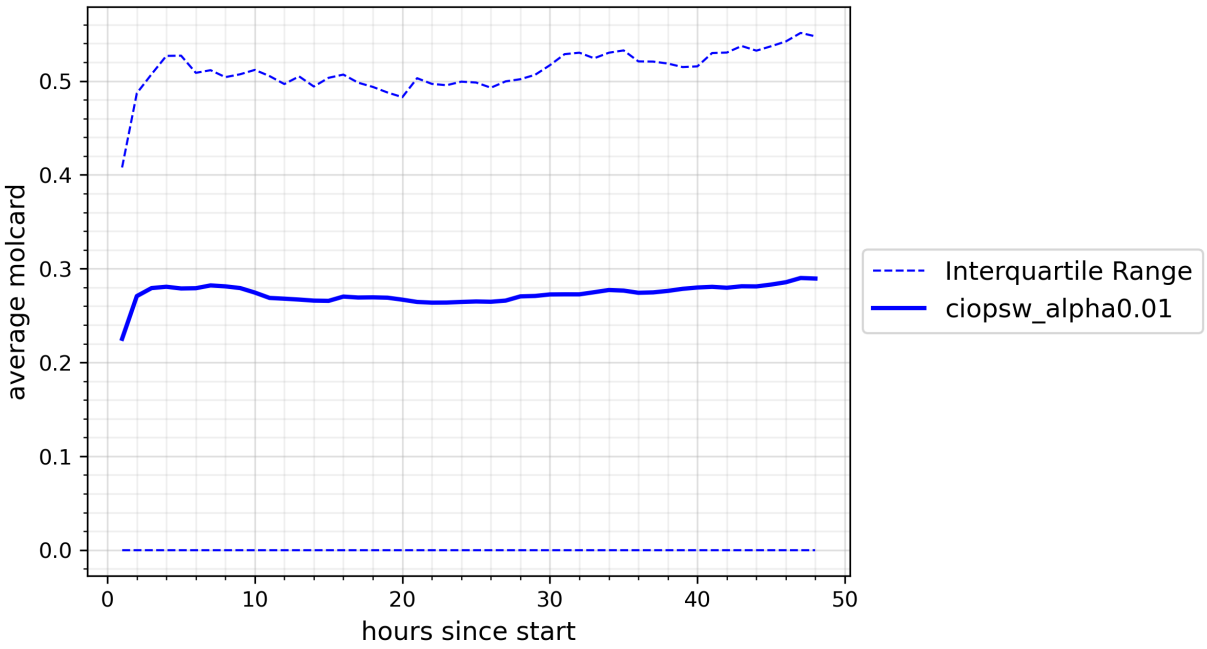

Figure 5: Average Molcard skill score (solid line) as a function of time since modelled drifter was released for all tracks shown in Figure 3. The dashed lines represent the 25th and 75th percentiles of the distribution.

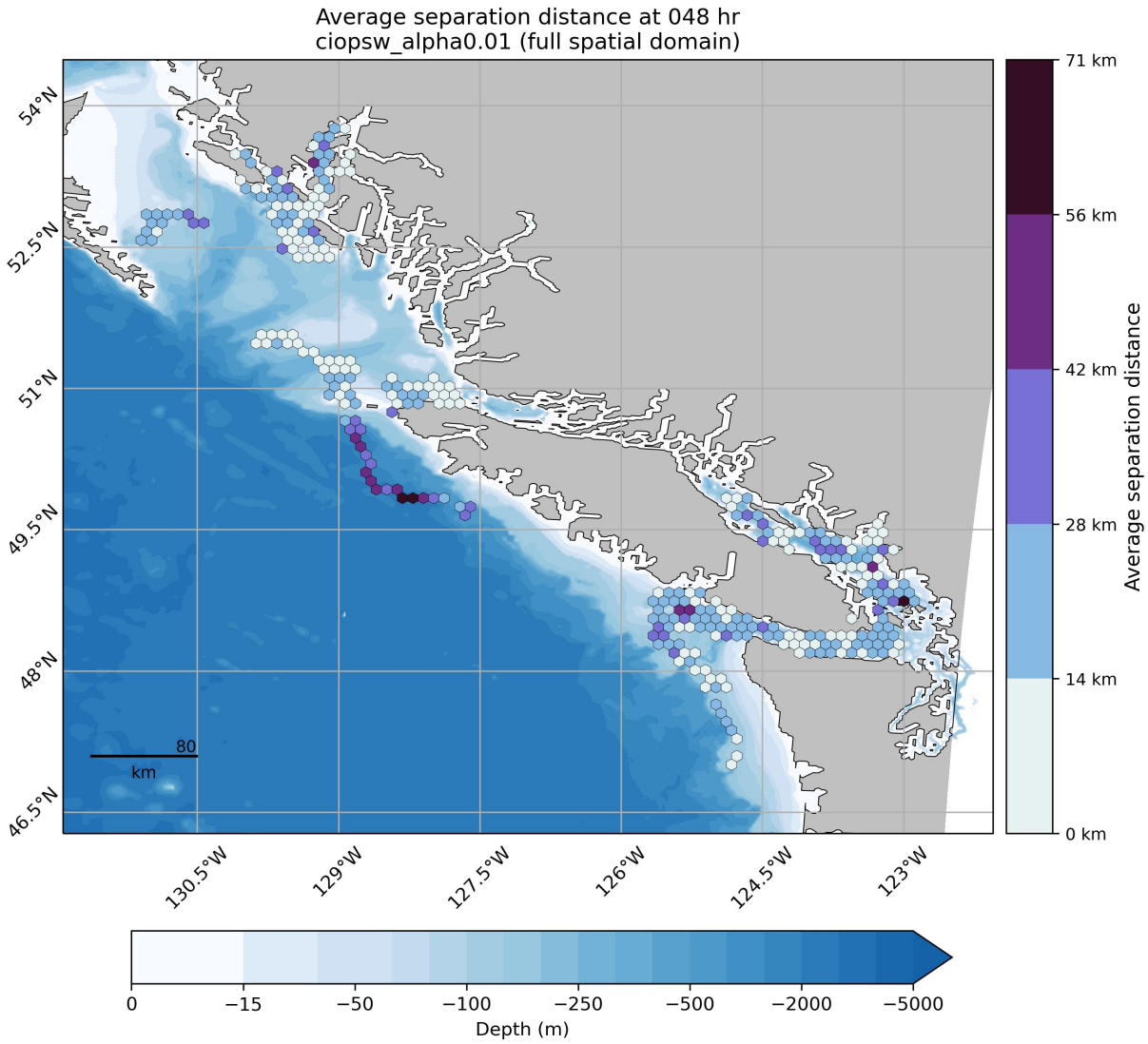

Figure 6: Average separation distance at time $t = 48$ hr binned spatially by model release location. Scores are shown for all tracks in Figure 3.

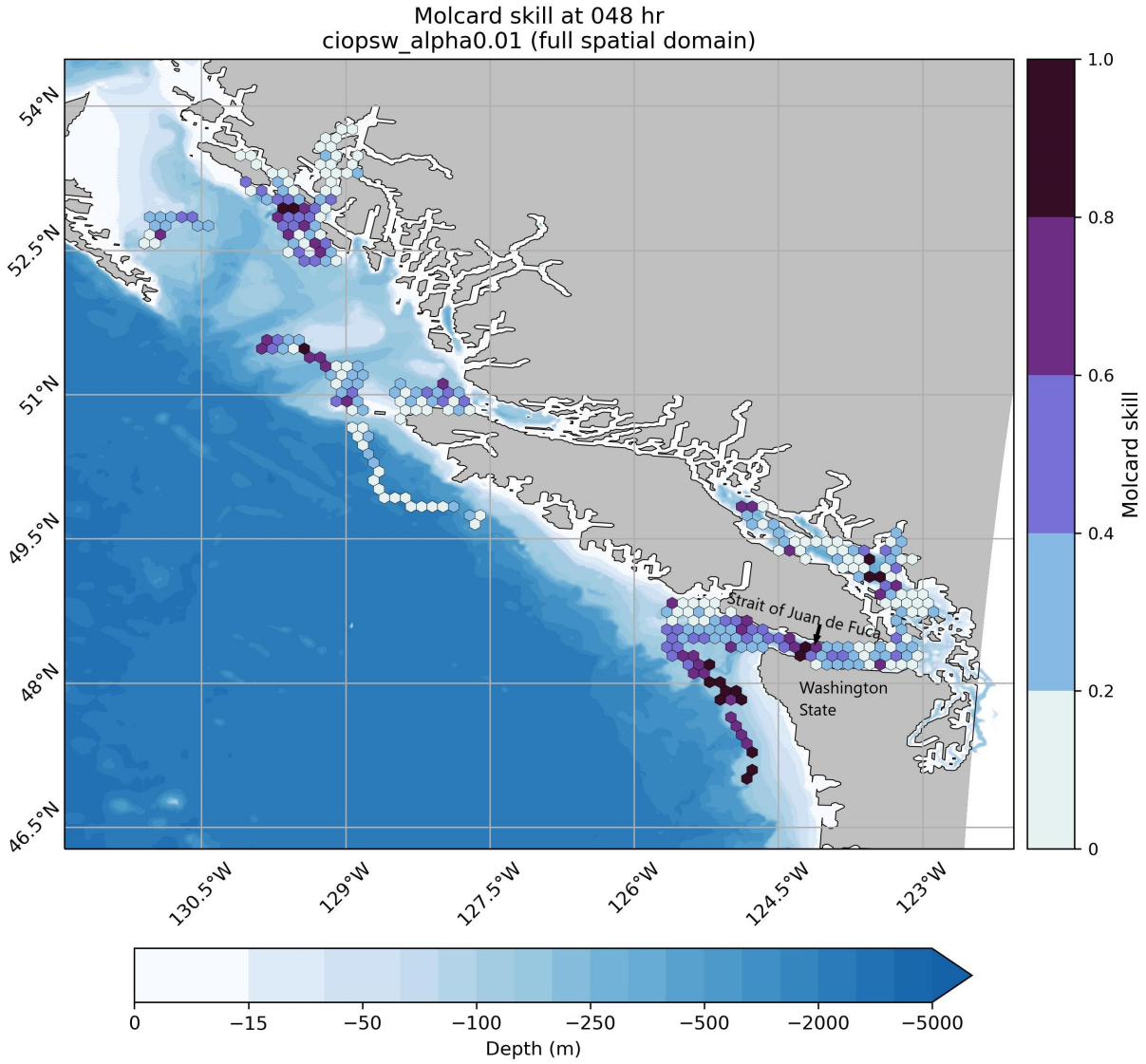

Figure 7: Average Molcard skill score at time $t = 48$ hr binned spatially by model release location. Scores are shown for all tracks in Figure 3. Locations were manually added to the plot in a separate program.

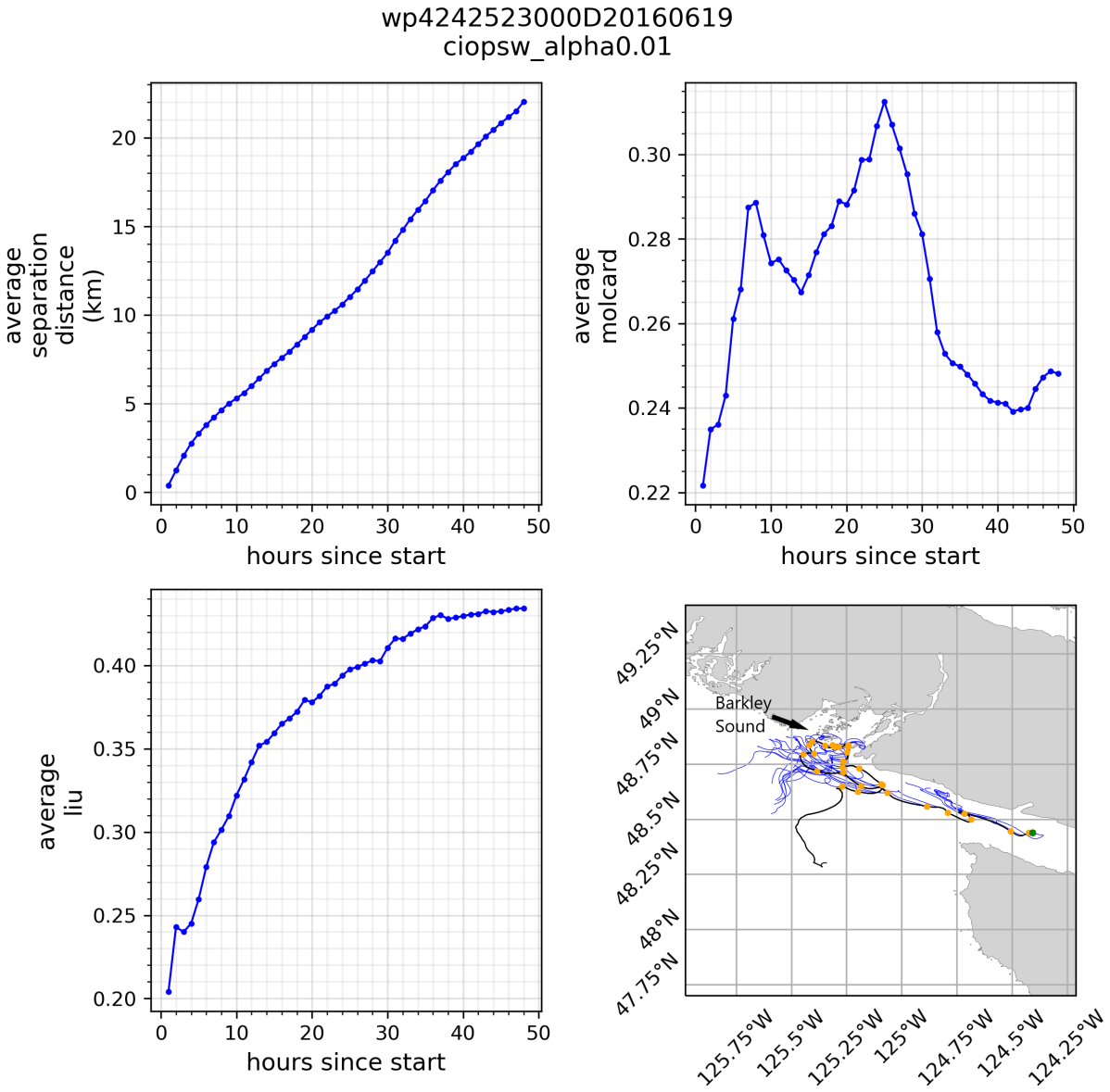

Figure 8: Average separation distance, Molcard skill score, and Liu skill score as a function of time since model release for a single drifter track shown in the map on the bottom right. The green dot is the observed drifter release point, the black line is the observed drifter track, the orange dots are the model initial positions and the blue lines are the model trajectories. In the title, wp4242523000D20160619 represents the drifter ID and ciopsw_alpha0.01 is a user defined identifier for the experiment. Locations were manually added to the plots in a separate program.

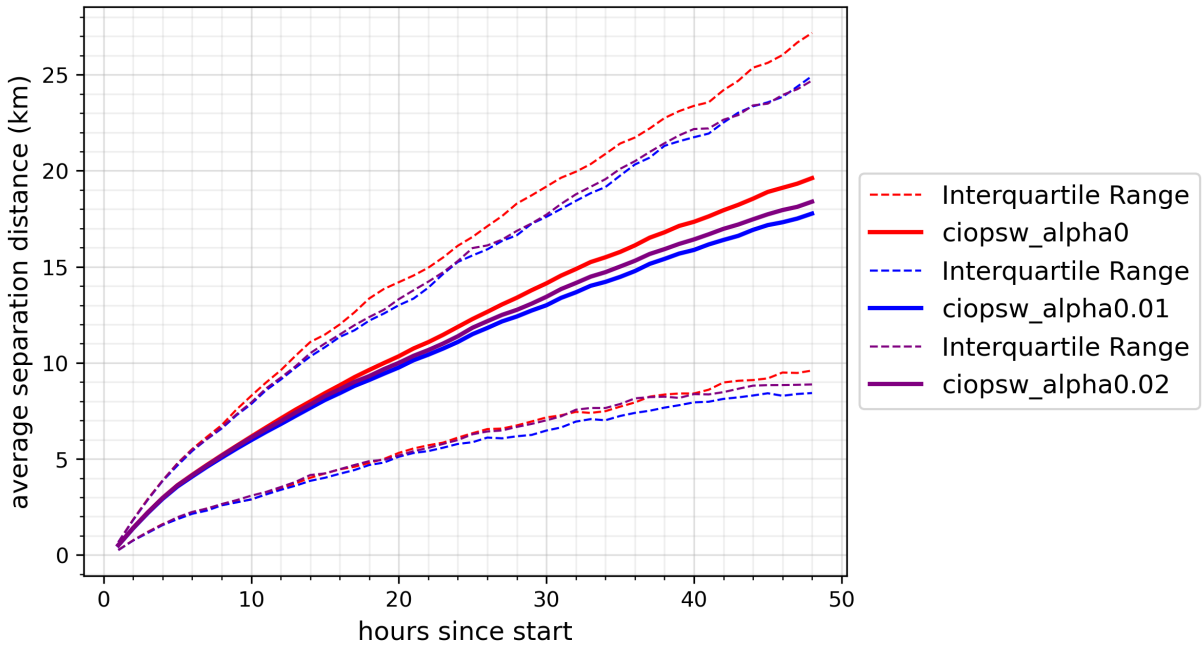

Figure 9: Average separation distance (solid lines) as a function of time since model release for all three experiments over the entire domain. The dashed lines represent the 25th and 75th percentiles of each distribution. The experiments are $\alpha = 0$ (red), $\alpha = 0.01$ (blue), and $\alpha = 0.02$ (purple) with winds from the HRDPS atmospheric model and surface currents from the CIOPS-W ocean model.

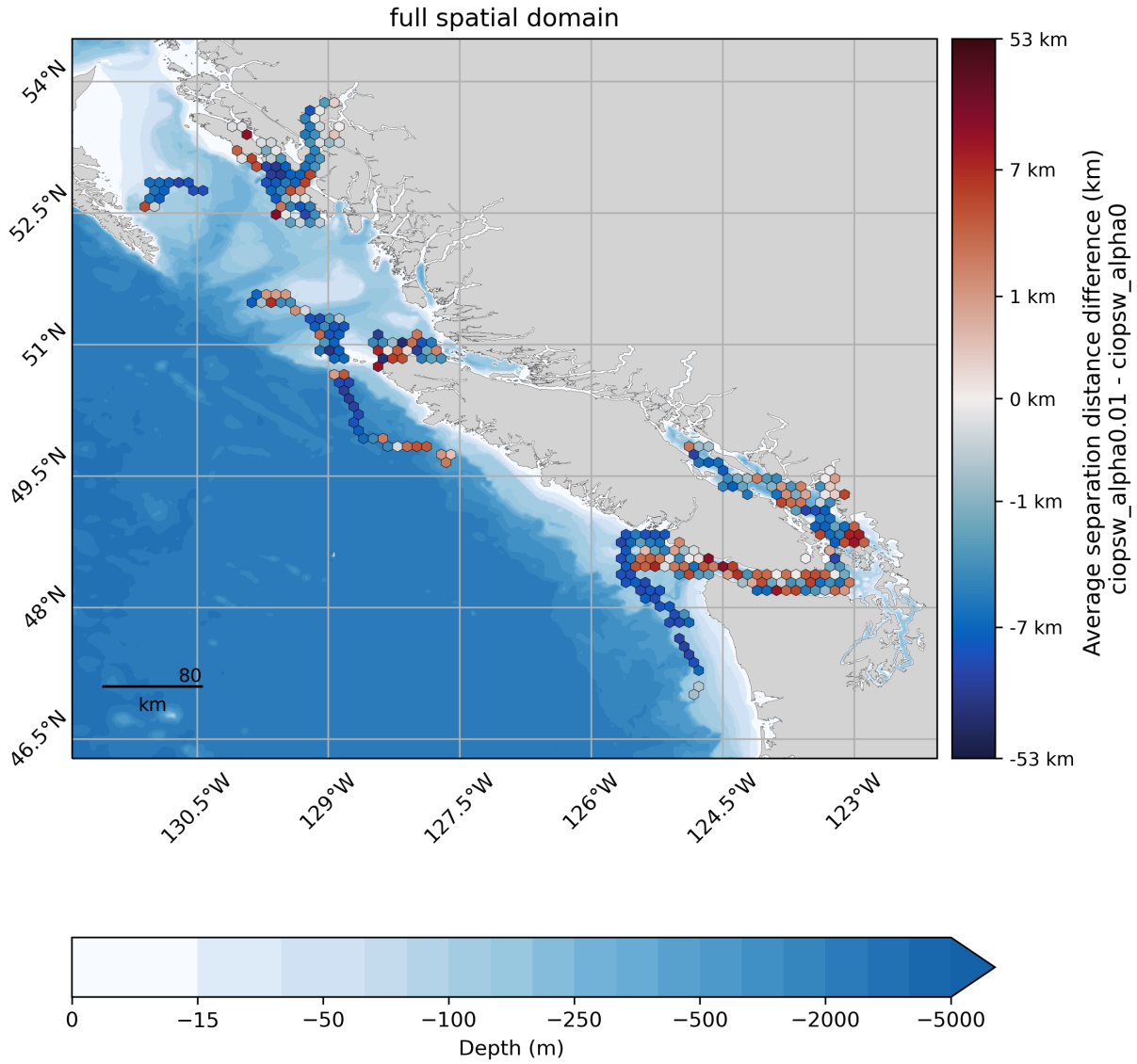

Figure 10: Difference in average separation distance at $t = 48$ hr for two experiments: $\alpha = 0.01$ subtract $\alpha = 0$.

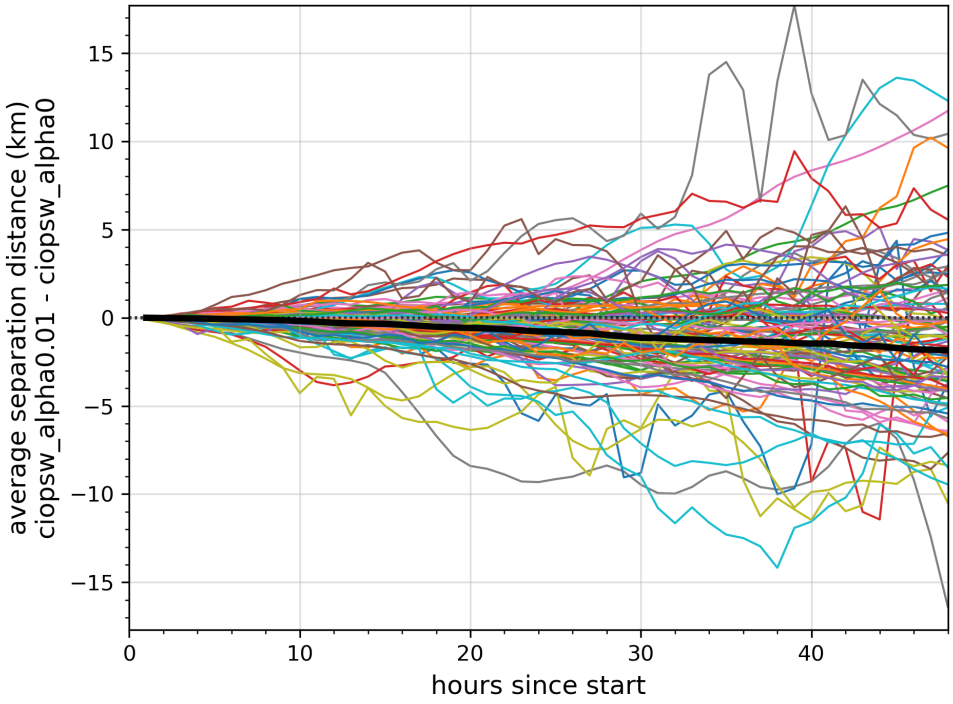

Figure 11: Difference in average separation distance as a function of time for two experiments: $\alpha = 0.01$ subtract $\alpha = 0$. Each drifter is shown as a separate line. The solid black line is the average across all drifters and the dotted line is $y = 0$.

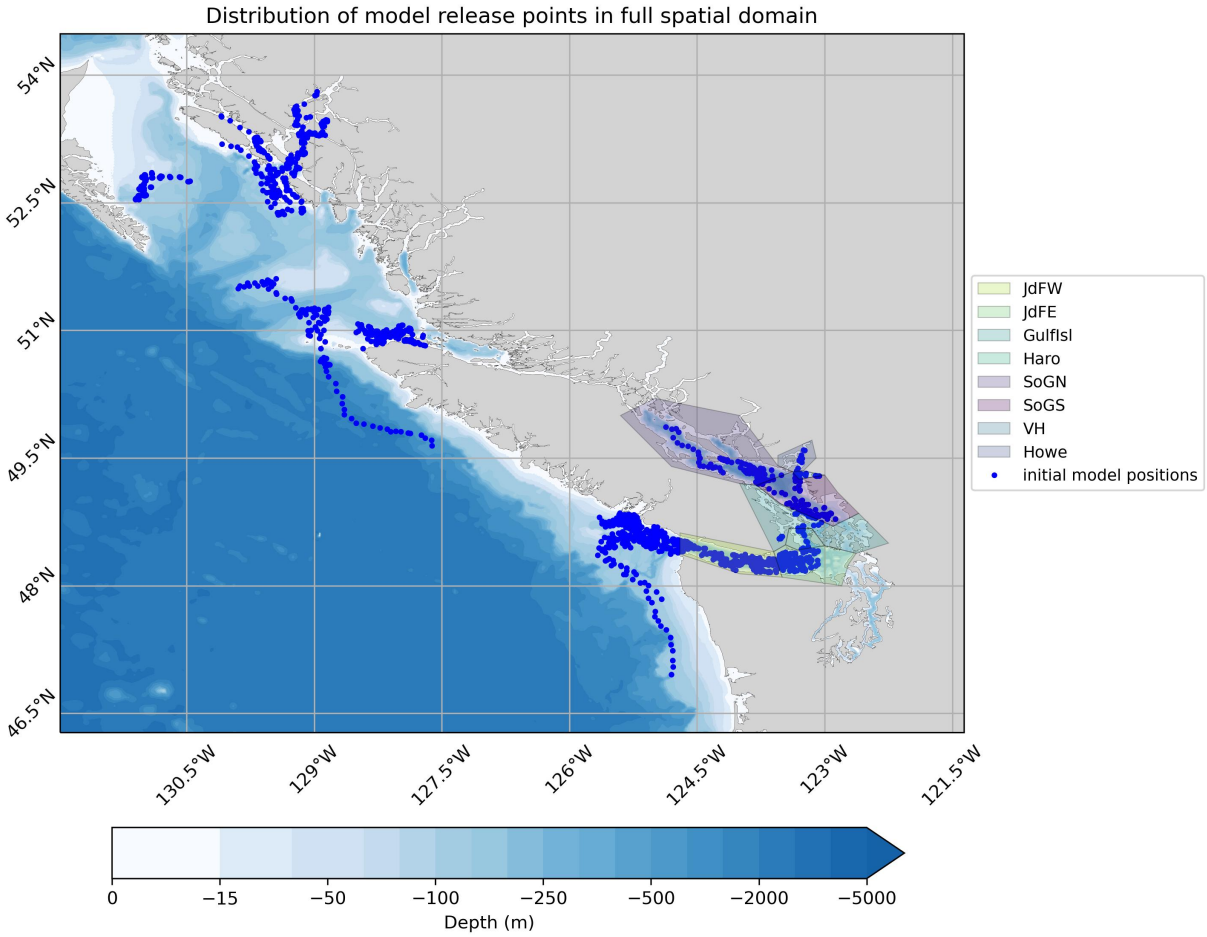

Figure 12: Definition of regions used in the regional comparison analysis. Blue dots are starting locations of all modelled drifters.

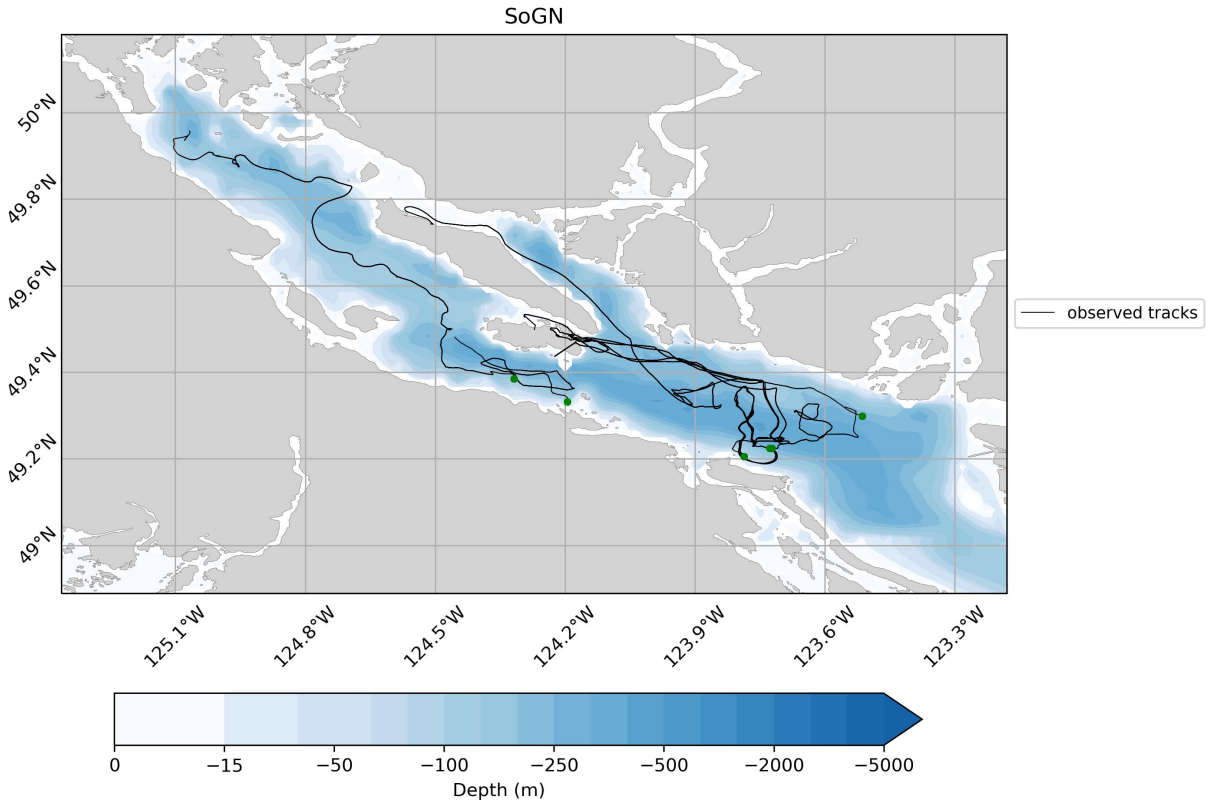

Figure 13: Straight of Georgia North observed drift tracks.

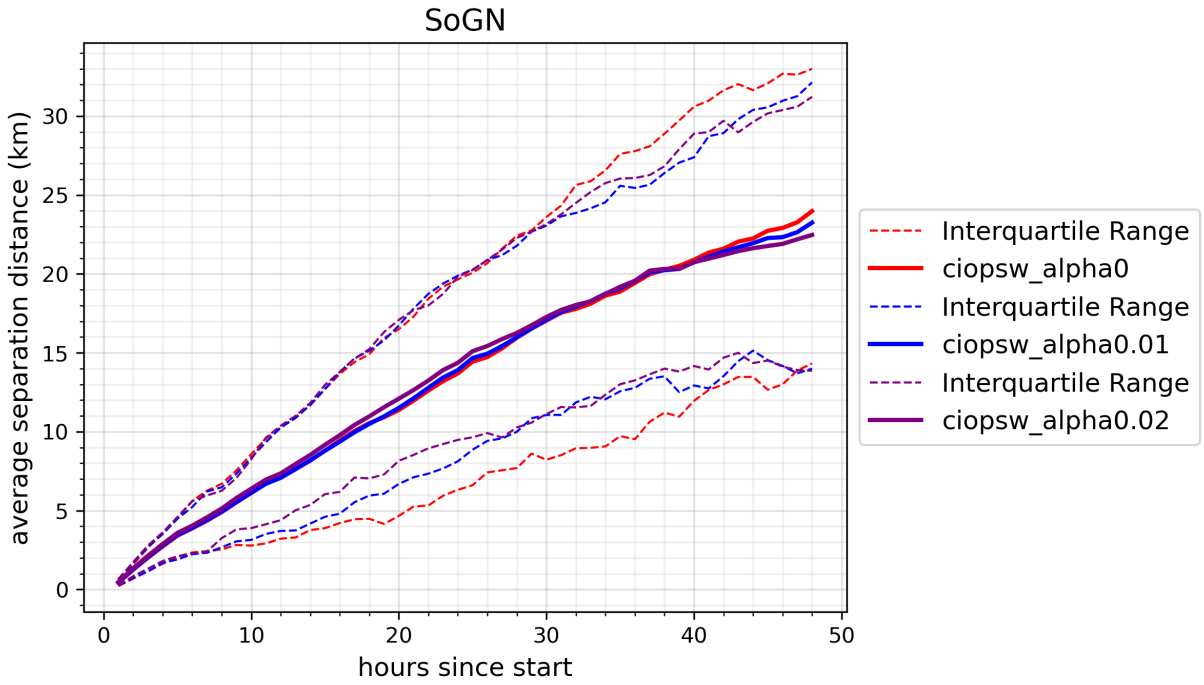

Figure 14: Average separation distance (solid lines) as a function of time since the modelled drifter was released for all tracks released in the SOGN region. The dashed lines represent the 25th and 75th percentiles of each distribution. The experiments are $\alpha = 0$ (red), $\alpha = 0.01$ (blue), and $\alpha = 0.02$ (purple) with winds from the HRDPS atmospheric model. Surface currents from the CIOPS-W model were used in all experiments.

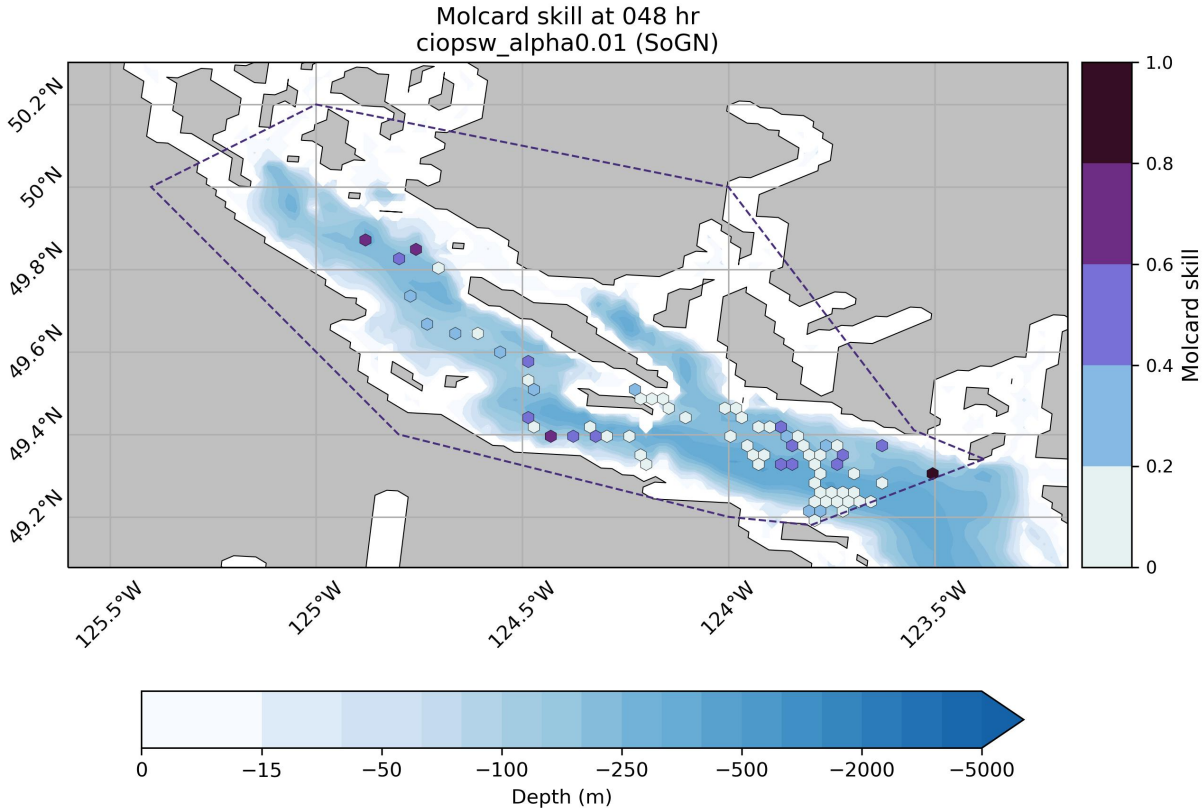

Figure 15: Average Molcard skill score at time $t = 48$ hr binned spatially by model release location. Scores are shown for all tracks released in the SoGN region and for the experiment with surface currents from the CIOPS-W ocean model and winds from the HRDPS atmospheric model with $\alpha = 0.01$.

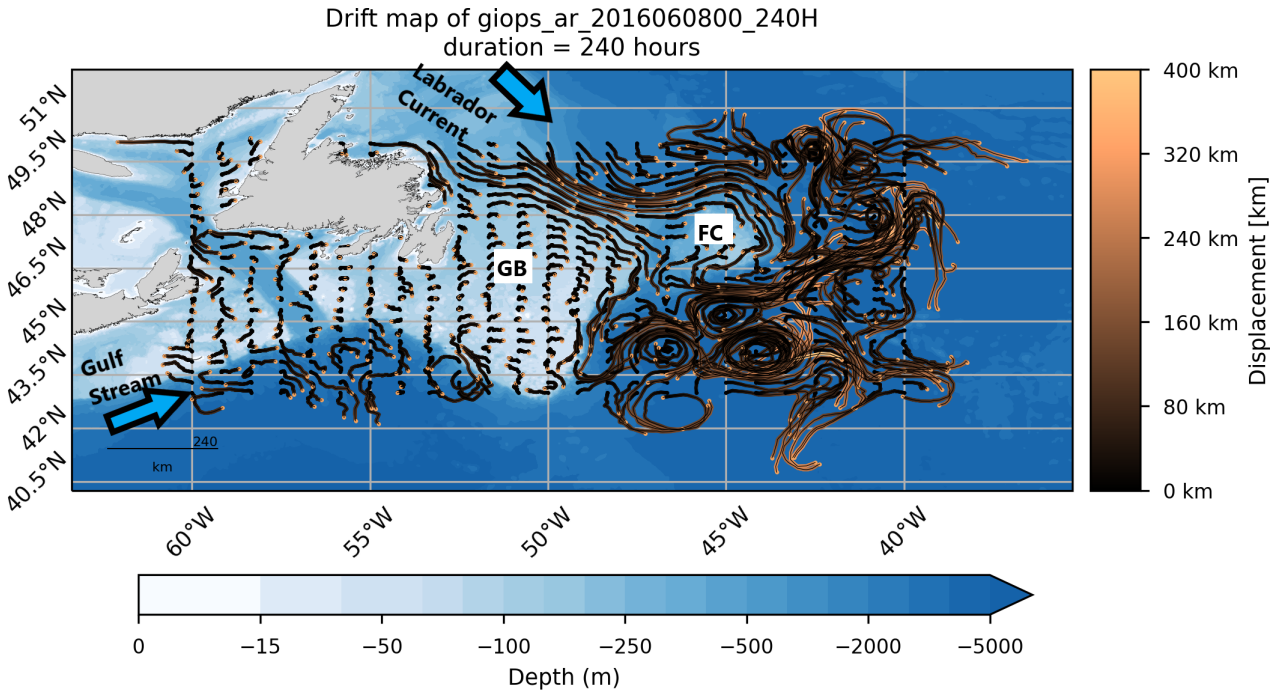

Figure 16: Trajectories of a grid of 25 x 25 particles forced by the GIOPS ocean model currents at 15 m depth for a duration of 10-days. Trajectories are coloured by the total distance travelled at each point along its path. Prominent currents such as the Labrador Current and Gulf Stream are marked by the blue arrows. Geographical locations such as Grand Banks (GB) and Flemish Cap (FC) are marked as well. Currents and locations were manually added to the plot in a separate program. In the title, giops_ar_2016060800_240H indicates that the run used the GIOPS ocean model, the Ariane (ar) drift methodology, and the particles were initialized on 20160608 and plotted after a duration of 240 hours (240H).

.

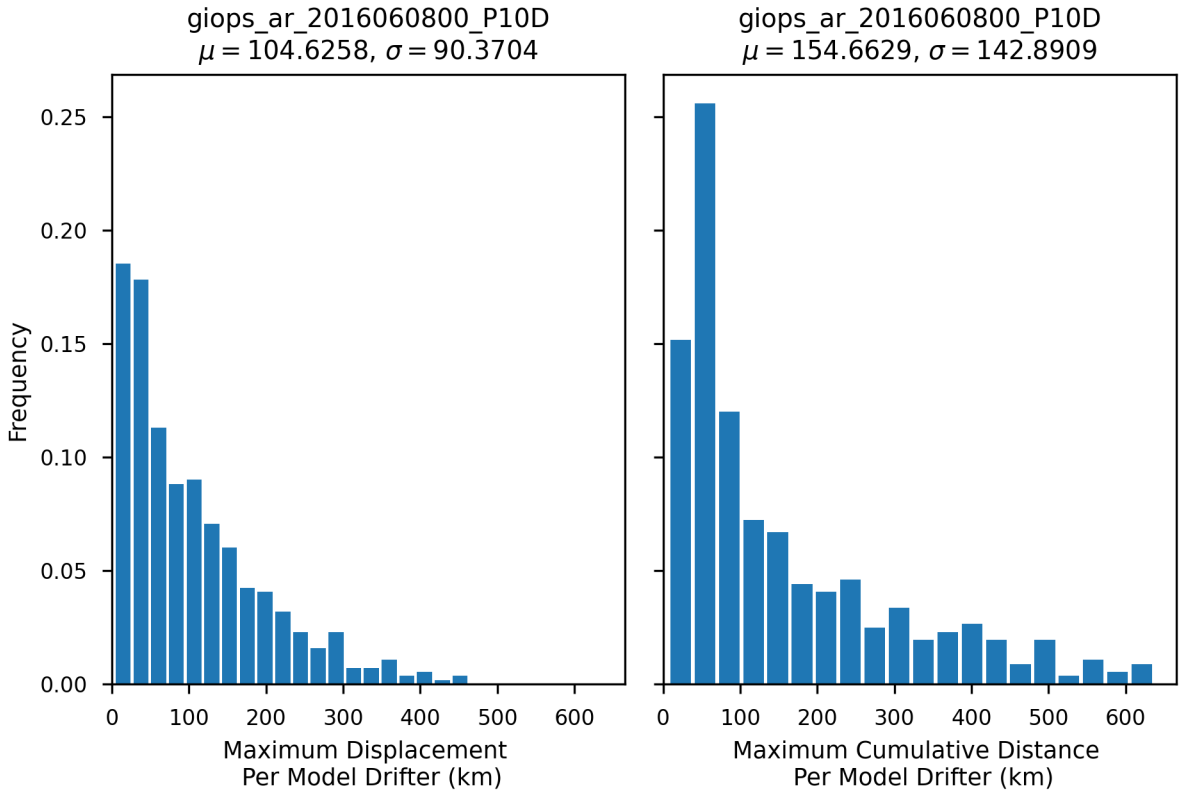

Figure 17: Histogram of the maximum displacement (left) and maximum distance travelled (right) for the trajectories shown in Figure 16. The mean (μ) and standard deviation (σ) of each distribution are printed in the title. Also, giops_ar_2016060800_P10D indicates that the run used the GIOPS ocean model, the Ariane (ar) drift methodology, and the particles were initialized on 20160608 and released for 10 days (P10D).

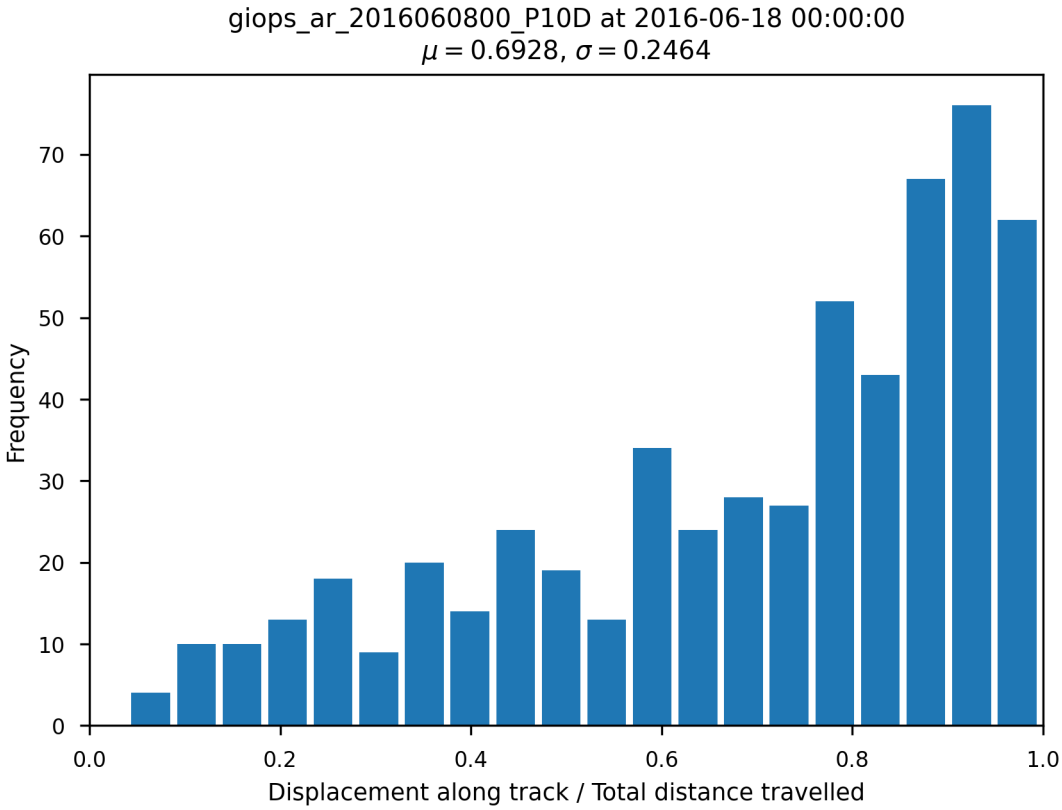

Figure 18: Histogram of the ratio between the displacement from origin and the total distance travelled for the trajectories shown in Figure 16. The mean (μ) and standard deviation (σ) of the distribution is printed in the title. Also, giops_ar_2016060800_P10D indicates that the run used the GIOPS ocean model, the Ariane (ar) drift methodology, and the particles were initialized on 20160608 and released for 10 days (P10D).

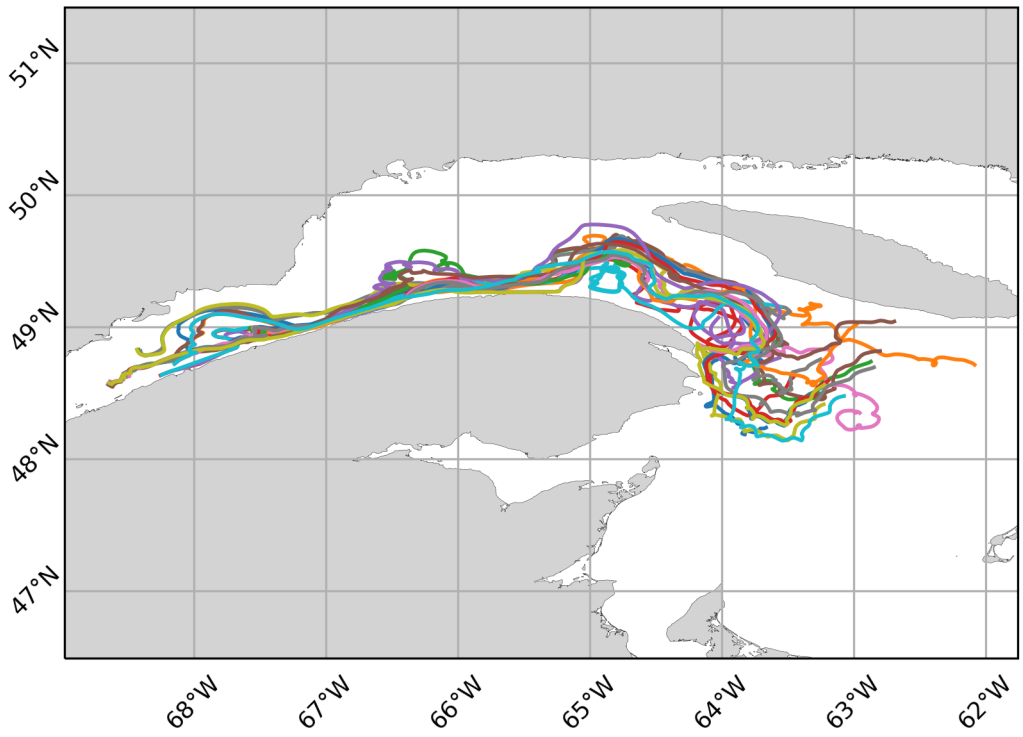

Figure 19: Trajectories of 20 Osker drifters released in the St. Lawrence Estuary in September 2020 as part of TReX.

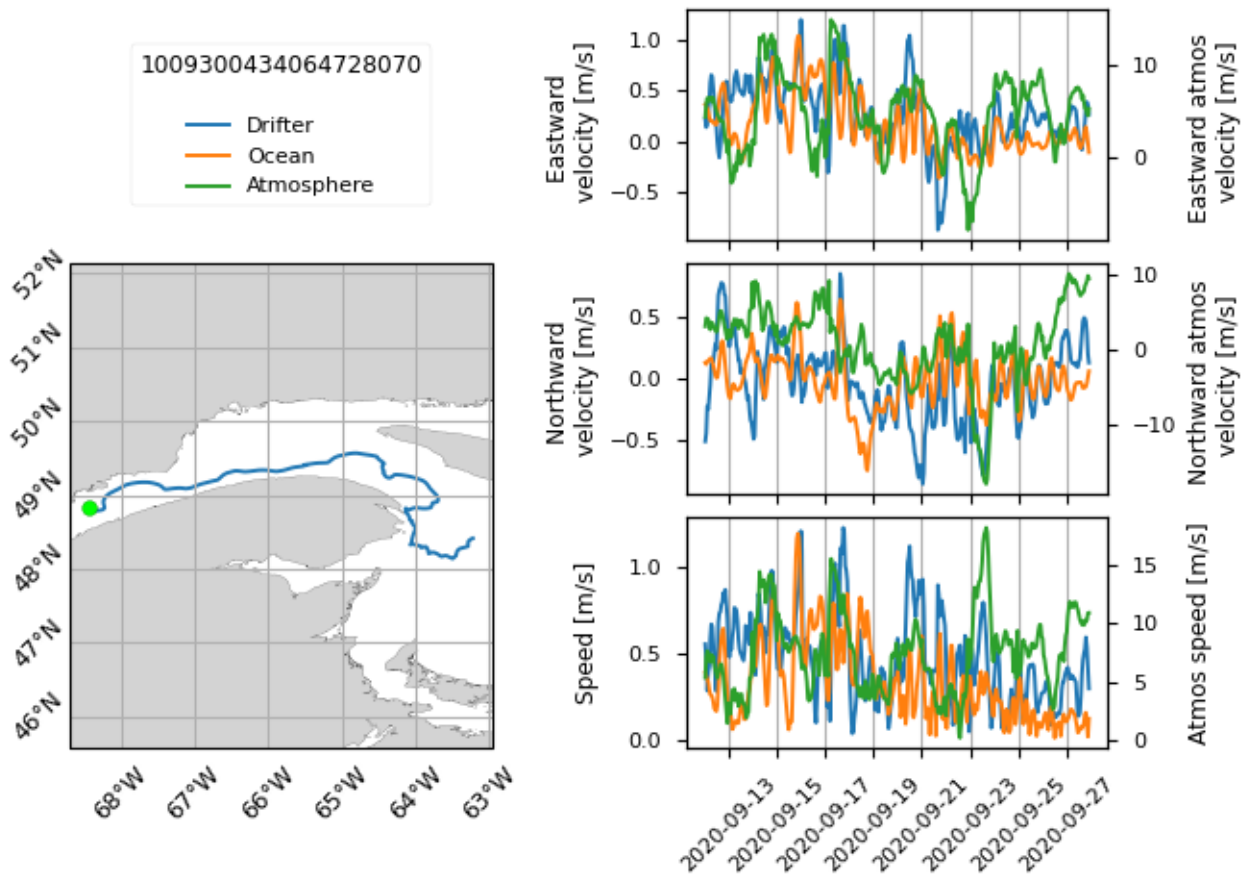

Figure 20: Trajectory of a single drifter from the group shown in Figure 19 (left). The green dot represents the release location of the drifter. Time series (right) of the drifter (blue), ocean (orange), and atmosphere (green) eastward velocity (top), northward velocity (middle), and speed (bottom). The CIOPS-E ocean model and the HRDPS atmosphere model were used. The drifter ID is 1009300434064728070.

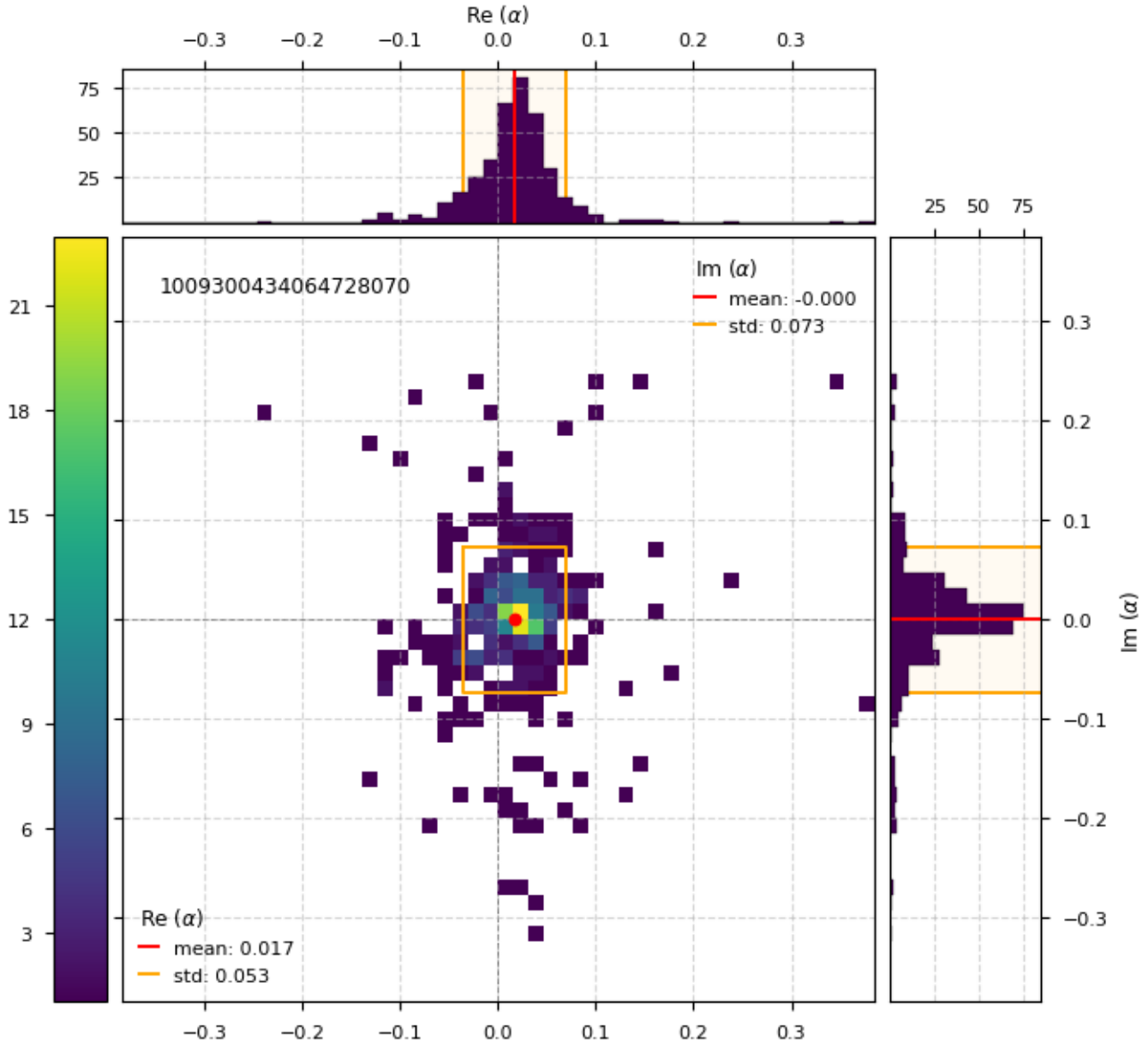

Figure 21: Example of the distribution of $\boldsymbol{\alpha}$ for the drifter shown in Figure 20. The two-dimensional histogram represents the real part of $\boldsymbol{\alpha}$ on the x-axis and the imaginary part of $\boldsymbol{\alpha}$ on the y-axis. One-dimensional histograms for each are shown in the top and right insets. Mean values are shown in red and standard deviations in yellow. The drifter ID is 1009300434064728070

.

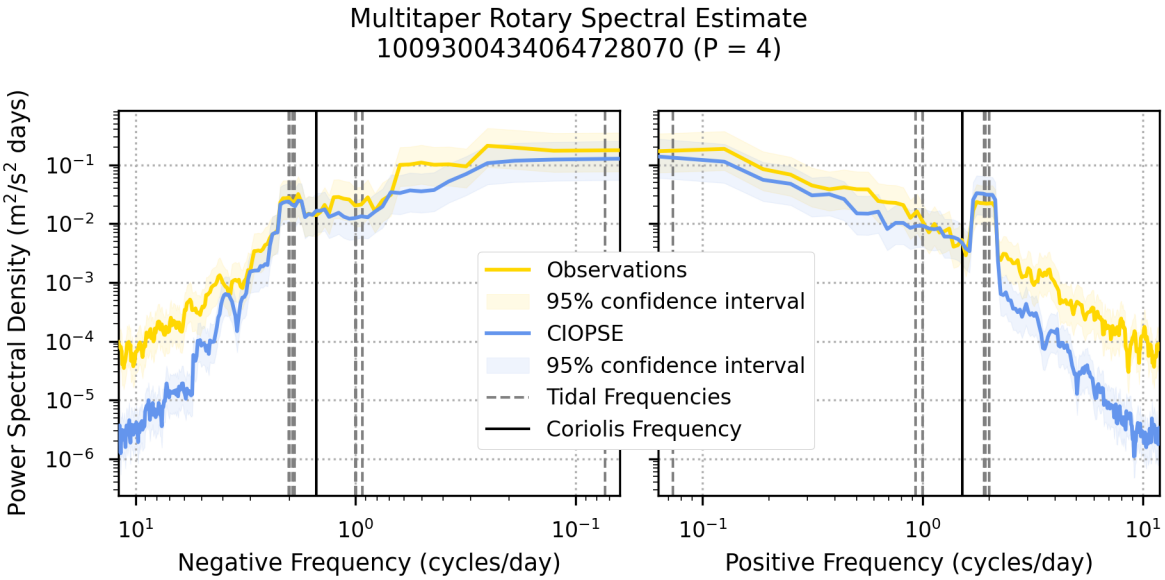

Figure 22: Rotary spectral estimate for the drifter velocity (yellow) and ocean model velocity (blue) for the drifter shown in Figure 20. The major diurnal and semi-diurnal tidal frequencies are shown in the gray dashed lines and the mean Coriolis frequency is in solid black. Negative frequencies (clockwise rotations) are on the left and positive frequencies (counterclockwise rotations) are on the right. The drifter ID is 1009300434064728070.

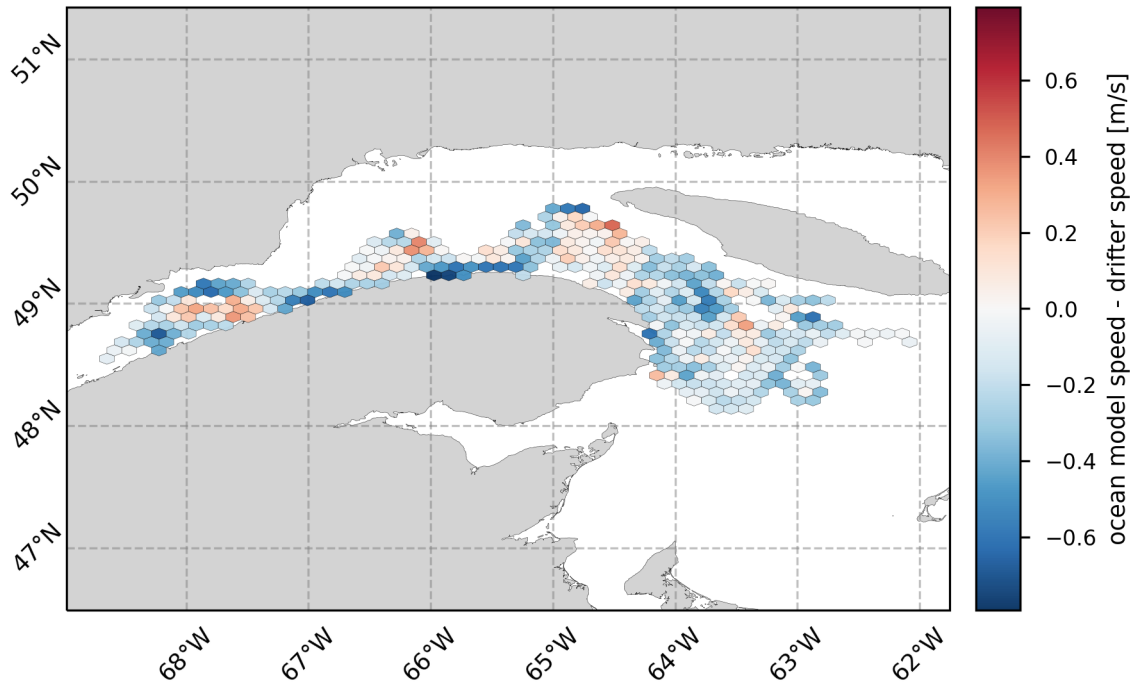

Figure 23: Average difference between ocean model speed and speed from the TReX drifters.

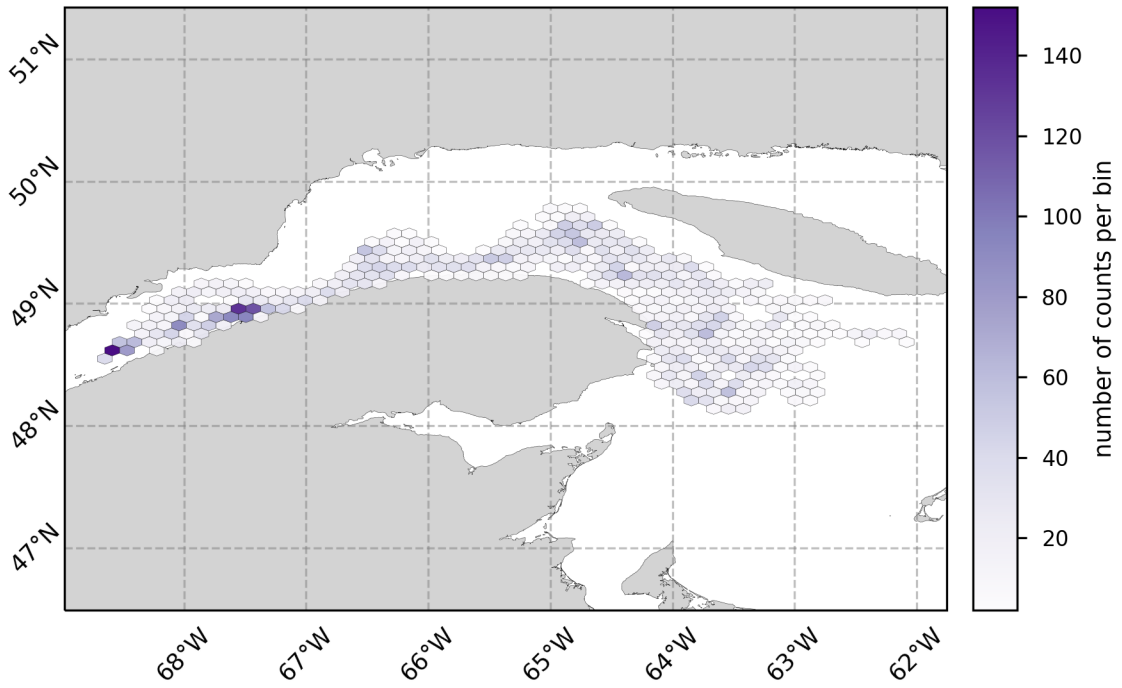

Figure 24: Histogram of the number of data points in each cell shown in Figure 23.

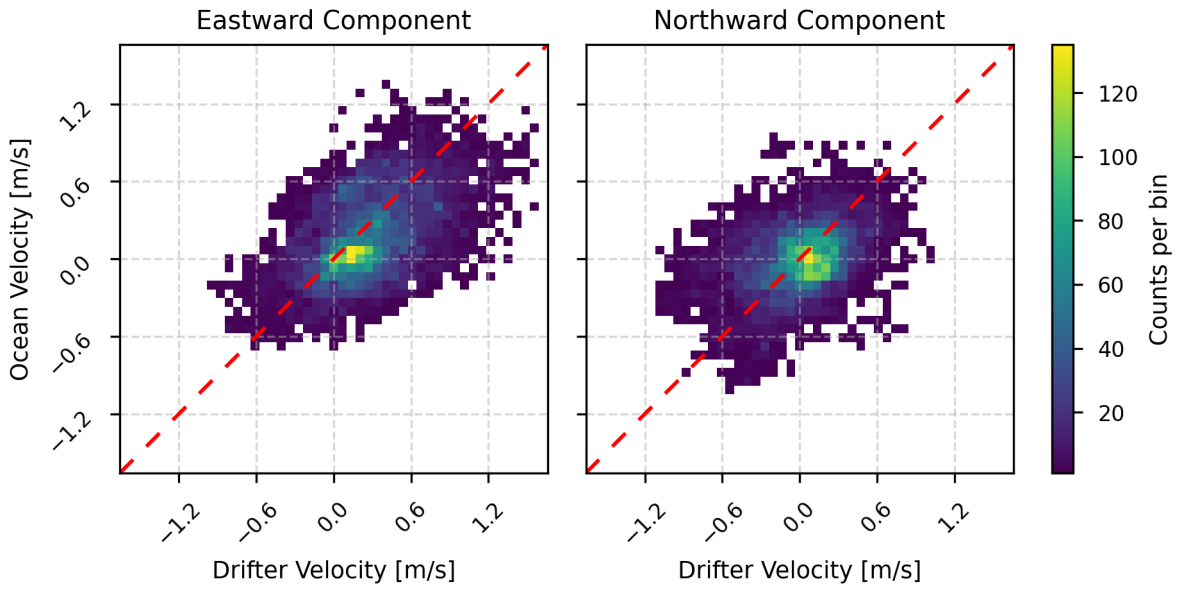

Figure 25: Two-dimensional histogram comparing the observed drifter and ocean model eastward (left) and northward (right) velocities. The CIOPS-E ocean model was used. The dashed red lines indicate where data points would be placed if there is a one-to-one correspondence between the model and drifters.